Table 2 Clinicopathological data in 13 patients developing interstitial pneumonia

Case	Age	Sex	Histology	Stage	Duration from start of therapy (days)	Status at onset	Symptom
1	62	F	DLBCL	I A	83	CR	No
2	75	F	DLBCL	I A	89	CR	No
3	83	F	DLBCL	II A	60	PR	Dyspnea
4	81	F	DLBCL	I B	78	PR	Dyspnea
5	67	F	DLBCL	II A	102	CR	Fever
6	60	F	DLBCL	II A	83	CR	No
7	42	M	DLBCL	IV A	158	CR	Fever
8	75	F	DLBCL	II A	78	CR	Fever
9	71	F	DLBCL	IV A	99	NC	Fever
10	64	M	FL	IV A	62	PR	Fever
11	70	M	DLBCL	I A	71	PR	Fever
12	36	F	DLBCL	I A	96	CR	Fever
13	61	M	DLBCL	I A	60	CR	Dyspnea

M male, *F* female, *DLBCL* diffuse large B-cell lymphoma, *FL* follicular lymphoma, *CR* complete response, *PR* partial response, *NC* no change, *ND* not done

patients, and low in four patients. In 5 of 13 patients, IP occurred within 10 days of the completion of granulocyte colony-stimulating factor (G-CSF) therapy. Serum LDH levels were above normal in 12 patients, and the KL-6 level was above normal in 6 of 10 patients examined (Table 3).

Among R-CHOP-treated patients, the serum level of β-D-glucan was above normal (~10 pg/ml; range 20.2–130.8 pg/ml) in 8 of 12 (75%) IP patients examined, and negative in all 30 non-IP patients assessed. All IP patients were negative for *Candida* and *Aspergillus* antigens in peripheral blood. Furthermore, 11 patients tested were negative for CMV antigenemia, adenovirus, and *Klebsiella* antigens, and *Mycoplasma* antibodies. In five patients whose sputum was examined, *P. jirovecii* DNA was detected by the polymerase chain reaction in two patients, and *Candida albicans* was detected by culture in another two patients.

In 12 patients with IP, the serum IgG level was monitored every 2 months. Prior to treatment, the median serum IgG level was 1,193 mg/dl (range 832–1,736) and within the normal range in 11 of 12 patients, and the median serum IgG level at the onset of IP was 794.5 mg/dl (range 572–1,082) and below the normal range (820–1,700 mg/dl) in 10 (83.3%) of 12 patients.

For IP treatment, we used steroids, ST, and antifungals in the majority of patients. All patients responded well to treatment, and recovered within 2–3 weeks. The changes in β-D-glucan, CRP, and LDH are shown in Table 4. After recovery from IP, five patients received R-CHOP therapy and four underwent radiotherapy while receiving antifungal and anti-PCP treatment. No patient experienced recurrence of IP.

4 Discussion

Several studies have reported an association between IP and rituximab-combined chemotherapy. However, there have been no prospective studies on this adverse event, and the etiology remains unclear. Herein, we compared the incidence of IP in patients with B-cell NHL treated by R-CHOP with that in patients treated by CHOP alone. There were no cases of IP among patients treated with CHOP, whereas 13 of 90 (14.3%) patients treated with R-CHOP developed IP, although there were no significant differences in baseline data between the two treatment groups.

Among patients treated with R-CHOP examined regarding their serum level of β-D-glucan, it was increased in 8 (cases 4, 5, 6, 7, 9, 10, 12, and 13) of 12 (75%) IP patients compared with none of 30 non-IP patients as a control. Among five IP patients undergoing sputum examination, *P. jirovecii* was positive in two by the polymerase chain reaction and *C. albicans* was positive in another two, one (case 8) of whom was β-D-glucan-negative. G-CSF was suspected to be the cause of IP in case 9 as IP developed during G-CSF administration with a sudden increase in the leukocyte count, as has been reported [10, 11]. In our study, fever and itching were noted during the first rituximab infusion in 6 of 13 patients. Two (cases 1 and 2) of them were negative for β-D-glucan, and, thus, possibly developed rituximab-induced lung injury during the succeeding rituximab infusion, because it has been reported to develop during the second or later administration in patients showing an allergic reaction on the first infusion [4, 7]. In two patients (cases 3 and 11), we did not identify the cause of the IP.

β-D-glucan has emerged as an adjunctive diagnostic measurement for PCP and invasive fungal infection, although an increase in serum β-D-glucan does not directly lead to a diagnosis of PCP or fungal infection [12–14]. In two patients with IP, PCP was diagnosed by detecting *P. jirovecii* DNA in sputum, which is known to be a less sensitive specimen than bronchoalveolar lavage or

Table 3 Clinical, biochemical data in 13 patients developing interstitial pneumonia

Case	Serum beta-D glucan (pg/ml)	Culture of sputum	LDH (U/l)	KL-6 (U/ml)	WBC count at onset (/μl)	Duration from G-CSF therapy	Infusion reaction	Treatment
1	Negative	ND	395	388	1,600	ND	Yes	mPSL 250 mg, FLCZ, ST
2	Negative	ND	445	832	5,500	14 days	Yes	mPSL 250 mg, FLCZ, ST
3	ND	ND	201	ND	1,700	ND	Yes	mPSL 250 mg, FLCZ, ST, CFPM
4	28.7	*C. albicans*	355	755	4,900	3 days	Yes	mPSL 250 mg, MKFG, CFPM
5	20.2	ND	367	390	2,800	4 days	No	mPSL 250 mg, CFPM
6	100.0	ND	329	ND	400	ND	No	PSL 60 mg, FLCZ, ST
7	50.6	Negative	543	335	4,800	4 days	No	MKFG, ST, CFPM, γ-globulin
8	Negative	*C. albicans*	378	ND	7,000	ND	No	VRCZ, CFPM
9	130.8	ND	489	500	12,800	During therapy	No	mPSL 250 mg, FLCZ, ST
10	48.5	PCP	347	421	4,200	ND	Yes	mPSL 250 mg, VRCZ, ST, CFPM
11	Negative	ND	253	686	10,700	ND	No	PSL 30 mg, ST, FLCZ
12	59.2	ND	450	531	6,500	ND	Yes	mPSL 1,000 mg, ST, FLCZ
13	65	PCP	580	748	6,500	4 days	No	mPSL 500 mg, ST, FLCZ

Infusion reaction indicates fever and itching during first rituximab administration

ND not done, *C. albicans Candida albicans*, *PCP Pneumocystis carinii* pneumonia, *WBC* white blood cell (4,000–8,000), *LDH* lactate dehydrogenase (−235), *KL-6* Klebsvonden Lungen-6 (−499), *G-CSF* granulocyte colony-stimulating factor, *PSL* prednisone, *mPSL* methylpredonisolone, *FLCZ* fluconazole, *ST* sulfamethoxazole-trimethoprim, *CFPM* cefepime dihydrochloride, *MKFG* micafungin sodium, *VRCZ* voriconazole

transbronchial lung biopsy. To clearly detect PCP, further investigations are required.

Recently, the incidences of PCP were reported to be 6 and 13% in patients treated with rituximab-combined bi-weekly CHOP with or without etoposide, respectively, while only 2 of 141 (1%) patients developed PCP following the conventional tri-weekly R-CHOP therapy. Although the authors did not clearly demonstrate the severe depletion of blood T lymphocytes, they suggested that dose-intensification and the addition of rituximab to CHOP-like regimens depleted the cellular immune system through the cytostatic effects of dose-intensified steroids and anti-cancer agents on lymphocytes, resulting in the development of PCP [8, 9]. They also showed that the addition of rituximab to CHOP-like regimens, such as CHOP and CHOP-14, with or without etoposide, increased the incidence of PCP [8]. Our results also suggest that the addition of rituximab to CHOP significantly increases the incidence of IP in patients with B-cell NHL, and some cases were possibly caused by *P. jiroveci* and fungal infection.

Table 4 The changes in clinical, biochemical data from onset of interstitial pneumonia to post treatment

Case	β-D-glucan (pg/ml)	CRP (mg/dl)	LDH (U/l)
1	Neg	0.3→0.1	395→230
2	Neg	0.1→0.1	445→213
3	ND	6.1→0.1	201→222
4	28.7→ND	10.3→0.2	355→277
5	20.2→Neg	0.3→0.1	367→233
6	100.0→Neg	1.9→0.1	329→200
7	50.6→Neg	12.4→0.3	543→357
8	Neg	12.9→0.3	378→229
9	130.8→Neg	4.0→1.8	489→211
10	48.5→Neg	10.0→0.1	347→194
11	Neg	1.1→0.1	253→208
12	59.2→Neg	5.6→0.3	261→252
13	65→Neg	0.2→0.1	580→203

Onset→after treatment for interstitial pneumonia

Neg negative, *ND* not done *CRP* C-reactive protein (−0.5), *LDH* lactate dehydrogenase (−235)

The incidence of IP in our study was unexpectedly high. A previous report indicated that lung injury induced by rituximab alone or in combination with chemotherapy account for less than 0.03% among over 300,000 patients worldwide [2]. On the other hand, other authors reported a lung injury rate of 11% during R-CHOP therapy [1], and a study of rituximab plus bleomycin-containing chemotherapy identified an increased incidence of lung injury through adding rituximab to chemotherapy [15]. These studies did not provide details of lung injury and the incidence of IP. Onsets of IP in 12 of 13 cases in our analysis were in an outpatients setting, as for most patients included in other studies of R-CHOP. The reason for this phenomenon was not clear with these limited data, and, therefore, further investigations such as a multi-center study, or epidemiological approach will be necessary.

Another recent study also demonstrated that the rates of fungal infections were increased in patients treated with

R-CHOP compared with patients receiving CHOP alone. Since most of the infected patients were more than 80 years of age, the authors concluded that the addition of rituximab to CHOP increases the risk of fungal infection in a very elderly population [16]. However, the average age of our population was not remarkably higher than those in previous studies on R-CHOP, and the ages of populations in studies on PCP during R-CHOP-14 were similar to that in the current study [8, 9].

In conclusion, 13 of 90 (14%) patients treated with R-CHOP developed IP, compared with none of 105 patients receiving CHOP alone as a historical control. Although the etiology remains unclear, increased susceptibility to *P. jirovecii* and fungal infection is suggested. This suggests the need to administer prophylactic treatment with antifungals and ST during R-CHOP therapy. The possible increase in the incidence of IP should be kept in mind when CHOP is combined with rituximab, since the treatment outcome for IP on the use of steroids, ST, and antifungals was favorable.

References

1. Coiffier B, Lepage E, Briere J, et al. Chop chemotherapy plus rituximab compared with chop alone in elderly patients with diffuse large-b-cell lymphoma. N Engl J Med. 2002;346:235–42.
2. Burton C, Kaczmarski R, Jan-Mohamed R. Interstitial pneumonitis related to rituximab therapy. N Engl J Med. 2003;348:2690–1; discussion 2690–1.
3. Alexandrescu DT, Dutcher JP, O'Boyle K, Albulak M, Oiseth S, Wiernik PH. Fatal intra-alveolar hemorrhage after rituximab in a patient with non-Hodgkin lymphoma. Leuk Lymphoma. 2004;45:2321–5.
4. Saito B, Nakamaki T, Adachi D, Suzuki J, Tomoyasu S. Acute respiratory distress syndrome during the third infusion of rituximab in a patient with follicular lymphoma. Int J Hematol. 2004;80:164–7.
5. Swords R, Power D, Fay M, O'Donnell R, Murphy PT. Interstitial pneumonitis following rituximab therapy for immune thrombocytopenic purpura (itp). Am J Hematol. 2004;77:103–4.
6. Hiraga J, Kondoh Y, Taniguchi H, Kinoshita T, Naoe T. A case of interstitial pneumonia induced by rituximab therapy. Int J Hematol. 2005;81:169–70.
7. Herishanu Y, Polliack A, Leider-Trejo L, Grieff Y, Metser U, Naparstek E. Fatal interstitial pneumonitis related to rituximab-containing regimen. Clin Lymphoma Myeloma. 2006;6:407–9.
8. Kolstad A, Holte H, Fossa A, Lauritzsen GF, Gaustad P, Torfoss D. Pneumocystis jirovecii pneumonia in b-cell lymphoma patients treated with the rituximab-choep-14 regimen. Haematologica. 2007;92:139–40.
9. Brusamolino E, Rusconi C, Montalbetti L, et al. Dose-dense r-chop-14 supported by pegfilgrastim in patients with diffuse large b-cell lymphoma: a phase ii study of feasibility and toxicity. Haematologica. 2006;91:496–502.
10. Niitsu N, Iki S, Muroi K, et al. Interstitial pneumonia in patients receiving granulocyte colony-stimulating factor during chemotherapy: survey in Japan 1991–96. Br J Cancer. 1997;76:1661–6.
11. Nakase K, Tsuji K, Nagaya S, Tamaki S, Tanigawa M, Ikeda T, Miyanishi E, Shiku H. Acute interstitial pneumonitis during chemotherapy for haematological malignancy. Eur J Cancer Care (Engl). 2005;14:336–41.
12. Odabasi Z, Mattiuzzi G, Estey E, et al. Beta-D-glucan as a diagnostic adjunct for invasive fungal infections: validation, cutoff development, and performance in patients with acute myelogenous leukemia and myelodysplastic syndrome. Clin Infect Dis. 2004;39:199–205.
13. Kawazu M, Kanda Y, Nannya Y, et al. Prospective comparison of the diagnostic potential of real-time PCR, double-sandwich enzyme-linked immunosorbent assay for galactomannan, and a (1–>3)-beta-D-glucan test in weekly screening for invasive aspergillosis in patients with hematological disorders. J Clin Microbiol. 2004;42:2733–41.
14. Ostrosky-Zeichner L, Alexander BD, Kett DH, et al. Multicenter clinical evaluation of the (1–>3) beta-D-glucan assay as an aid to diagnosis of fungal infections in humans. Clin Infect Dis. 2005;41:654–9.
15. Ghesquieres H. Severe interstitial pneumonitis following rituximab and bleomycin-containing combination chemotherapy. Ann Oncol. 2005;16:1399.
16. Lin PC, Hsiao LT, Poh SB, et al. Higher fungal infection rate in elderly patients (more than 80 years old) suffering from diffuse large b cell lymphoma and treated with rituximab plus chop. Ann Hematol. 2007;86:95–100.

ELSEVIER

INSTITUT PASTEUR

Microbes and Infection 10 (2008) 748–756

www.elsevier.com/locate/micinf

Original article

Induction of apoptosis in Epstein-Barr virus-infected B-lymphocytes by the NF-κB inhibitor DHMEQ

Ariko Miyake [a,1], Md. Zahidunnabi Dewan [b,c,1], Takaomi Ishida [a], Mariko Watanabe [d], Mitsuo Honda [c], Tetsutaro Sata [e], Naoki Yamamoto [b,c,**], Kazuo Umezawa [f], Toshiki Watanabe [a,***], Ryouichi Horie [d,*]

[a] *Laboratory of Tumor Cell Biology, Department of Medical Genome Sciences, Graduate School of Frontier Sciences, University of Tokyo, 4-6-1 Shirokanedai, Minato-ku, Tokyo 108-8639, Japan*

[b] *Department of Molecular Virology, Bio-Response, Graduate School, Tokyo Medical and Dental University, 1-5-45 Yushima, Bunkyo-ku, Tokyo 113-8519, Japan*

[c] *AIDS Research Center, National Institute of Infectious Diseases, 1-23-1 Toyama, Shinjuku-ku, Tokyo 162-8640, Japan*

[d] *Department of Hematology, School of Medicine, Kitasato University, 1-15-1 Sagamihara, Kanagawa 228-8555, Japan*

[e] *Department of Pathology, National Institute of Infectious Diseases, 1-23-1 Toyama, Shinjuku-ku, Tokyo 162-8640, Japan*

[f] *Department of Applied Chemistry, Faculty of Science and Technology, Keio University, 3-14-1 Hiyoshi, Kohoku-ku, Yokohama, Kanagawa 223-0061, Japan*

Received 19 January 2008; accepted 9 April 2008
Available online 13 April 2008

Abstract

Epstein–Barr virus (EBV) causes EBV-associated lymphoproliferative diseases in patients with profound immune suppression. Most of these diseases are life-threatening and the prognosis of AIDS-associated lymphomas is extremely unfavorable. Polyclonal expansion of virus infected B-cell predisposes them to transformation. We investigated the possibility of nuclear factor kappa B (NF-κB) inhibition by dehydroxymethylepoxyquinomicin (DHMEQ) for the treatment and prevention of EBV-associated lymphoproliferative diseases. We examined the effect of DHMEQ on apoptosis induction in four EBV-transformed lymphoblastoid cell lines as well as peripheral blood mononuclear cells infected with EBV under immunosuppressed condition. DHMEQ inhibits NF-κB activation in EBV-transformed lymphoblastoid cell lines and induces apoptosis by activation of mitochondrial and membranous pathways. Using an *in vivo* NOD/SCIDγc mouse model, we showed that DHMEQ has a potent inhibitory effect on the growth of lymphoblastoid cells. In addition, DHMEQ selectively purges EBV-infected cells expressing latent membrane protein (LMP) 1 from peripheral blood mononuclear cells and inhibits the outgrowth of lymphoblastoid cells. These results suggest that NF-κB is a molecular target for the treatment and prevention of EBV-associated lymphoproliferative diseases. As a potent NF-κB inhibitor, DHMEQ is a potential compound for applying this strategy in clinical medicine.

Keywords: Epstein–Barr virus infections; NF-κB; DHMEQ

1. Introduction

Epstein–Barr virus (EBV) is a member of the γ-herpesvirus family that infects more than 90% of the world population and initially establishes latency III infection in B lymphocytes [1]. Latency III infection is characterized by the expression of the entire array of EBV latency genes, including EBV nuclear proteins (EBNA1, -2, -3A, -3B, -3C, and -LP), integral latent membrane proteins (LMP1, -2A, and -2B), the BamA

* Corresponding author. Tel.: +81 42 778 8111; fax: +81 42 778 8441.
** Tel.: +81 3 5803 5178; fax: +81 3 5803 0124.
*** Tel.: +81 3 5449 5298; fax: +81 3 5449 5418.
E-mail addresses: yamamoto.mmb@tmd.ac.jp (N. Yamamoto), tnabe@ims.u-tokyo.ac.jp (T. Watanabe), rhorie@med.kitasato-u.ac.jp (R. Horie).
[1] These authors contributed equally to this work.

1286-4579/$ - see front matter © 2008 Elsevier Masson SAS. All rights reserved.
doi:10.1016/j.micinf.2008.04.002

rightward transcripts (BARTs), and small RNAs (EBERs). Immune response mediated by T-lymphocytes eliminates most latency III-infected cells; however, resting memory B lymphocytes provide a reservoir for latent virus. T-lymphocyte immunity to latency III-infected B lymphocytes persists for life and protects reactivation of latent virus from a reservoir [2].

However, in the absence of an effective immune response, reactivation of latent virus from a reservoir occurs and causes EBV-associated lymphoproliferative diseases. EBV-associated lymphoproliferative diseases occur with primary infection after transplantation or reactivation of latent virus as a consequence of immune suppression for organ transplantation and autoimmune diseases or acquired immune deficiency syndrome (AIDS) [3–6]. EBV-associated lymphoproliferative diseases are associated in the majority of cases with latency type III phenotype. The prognosis of EBV-associated lymphoproliferative diseases is variable; however, most of these are life-threatening and the prognosis of AIDS-associated lymphomas is extremely unfavorable, although introduction of highly active anti-retroviral treatment (HAART) decreased the incidence, increased the effectiveness of chemotherapy, and improved survival [5]. EBV infection of B-lymphocytes *in vitro* also results in latency III infection and sustained cell proliferation as lymphoblastoid cell lines (LCLs).

Activation of nuclear factor kappa B (NF-κB) has been connected with resistance against apoptosis and tumorigenesis [7]. Despite the diversity in clinical manifestations of EBV-associated lymphoproliferative diseases, strong and constitutive NF-κB activity is reported to be a common characteristic of this disease entity. LMP1 mimics signaling from tumor necrosis factor (TNF) receptor family members by association with tumor necrosis factor receptor-associated factors (TRAFs) and activates the IKK (IκB kinase)—NF-κB pathway [8].

NF-κB represents five cellular proteins: c-Rel, RelA (p65), RelB, NF-κB1 (p50 and its precursor p105), and NF-κB2 (p52 and its precursor p100). The IκB inhibitory proteins consist of IκBα, IκBβ, IκBε, IκBγ, and Bcl-3. NF-κB forms homo- or heterodimers and exists as an inactive complex with IκB regulatory proteins in the cytoplasm. Various signaling pathways converge into IKK-mediated degradation of IκB proteins and subsequent release of uncomplexed NF-κB, which then migrates into the nucleus and activates the transcription of target genes [9].

Dehydroxymethylepoxyquinomicin (DHMEQ) is a new NF-κB inhibitor that is a 5-dehydroxymethyl derivative of the novel compound epoxyquinomicin C that has a 4-hydroxy-5,6-epoxycyclohexenone structure like panepoxydone. Panepoxydone had been found to inhibit TNF-α-induced activation of NF-κB [10]. We have shown that DHMEQ inhibits NF-κB at the level of nuclear translocation [11].

In this study, to investigate the possibility of NF-κB inhibition by DHMEQ as a strategy for the treatment and prevention of EBV-associated lymphoproliferative diseases, we investigated the effect of DHMEQ on apoptosis induction in four EBV-transformed LCLs as well as peripheral blood mononuclear cells (PBMC) in the early phase of EBV infection, and further examined the molecular mechanism of DHMEQ-induced apoptosis.

2. Materials and methods

2.1. Cells

B95.8 EBV-transformed LCLs were established by infection of lymphocytes from four healthy donors with culture supernatants of the virus producer B95.8 line as described previously [12], and are indicated in the text by the first two letters of the name of each donor. In all experiments to test the effects of DHMEQ treatment, LCLs were maintained in RPMI 1640 medium supplemented with 10% fetal bovine serum (FBS).

2.2. Chemicals

DHMEQ is an NF-κB inhibitor that blocks nuclear translocation of NF-κB [11]. DHMEQ was dissolved with dimethylsulfoxide (DMSO). DHMEQ or DMSO was used for experiments at indicated concentrations. Bisbenzimide H 33342 fluorochrome (Hoechst 33342) was purchased from Calbiochem (Bad Soden, Germany).

2.3. Electrophoretic mobility shift analysis

Electrophoretic mobility shift analysis (EMSA) was carried out according to the methods described previously [13]. For detecting NF-κB binding, a double-stranded oligonucleotide containing the κB site of the promoter for the mouse H-2Kb class I major histocompatibility antigen gene was used as a probe [14]. The nucleotide sequence is 5′-GAT CCG GCT GGG AAT CCC CGC TGG GAA TCC CCA TCT A-3′. For control EMSA, a double-strand oligonucleotide containing Oct-1 consensus sequence (Promega, Madison, WI, USA) was used as a probe. Antibodies used for supershift assays were as follows: NF-κB p50 (C-19) goat polyclonal antibody, rabbit polyclonal antibody for NF-κB p65 (C-20) and RelB (C-19), and mouse monoclonal antibody for c-Rel (B-6) and NF-κB p52 (C-5) (all from Santa Cruz Biotechnology Inc., Santa Cruz, CA). A mouse IgG antibody (Sigma, St. Louis, MO) served as a control.

2.4. Cell viability assay

The effects of DHMEQ on cell viability were assayed by color reaction with a tetrazolium salt, WST-8(4-[3-(2-methoxy-4-nitrophenyl)-2-[4-nitrophenyl]-2*H*-5-tetrazolio]-1,3-benzene disulfonate sodium salt) (Cell Counting Kit-8; Dojindo Laboratories, Kumamoto, Japan). After incubation with DHMEQ or DMSO at the indicated concentrations and time points, cells were treated with Cell Counting Kit-8 according to the manufacturer's recommendations and the results were measured by a microplate reader (Bio-Rad, Richmond, CA) at a test wavelength of 450 nm and reference wavelength of 630 nm.

2.5. Analysis of apoptosis and caspase activities

To quantify apoptosis, cells were labeled with fluorescein isothiocyanate (FITC)-conjugated Annexin V (BD Biosciences, Palo Alto, CA), then subjected to flow cytometric analysis. For analysis of nuclear DNA fragmentation, the terminal deoxynucleotidyl transferase (TdT)-mediated dUTP nick end-labeling (TUNEL) assay was done according to the manufacturer's recommendations (DeadEnd Fluorometric TUNEL Systems; Promega). Cells were analyzed using a FACS Calibur flow cytometer (BD Biociences) and fluorescence microscopy. Activities of caspase-3, -8, and -9 were determined by using green fluorochrome-labeled inhibitors of caspases (FLICA)-3, -8, and -9 (FLICA Apoptosis Detection Kit; Immunochemistry Technologies, Bloomington, MN). Cells from LCLs were treated with 10 μg/ml of DHMEQ (+) or with DMSO alone (−) for 8 h and fixed on slides; active caspases were detected by FLICA-3, -8, and -9. For detection of nuclear DNA, cells were stained with Hoechst 33342 and photographed through a UV filter and an Olympus BX50F microscope (Olympus, Tokyo, Japan).

2.6. In vivo effects of DHMEQ on NOG mice inoculated with LCLs

NOG mice were purchased from the Central Institute for Experimental Animals (Kawasaki, Japan). The Ethical Review

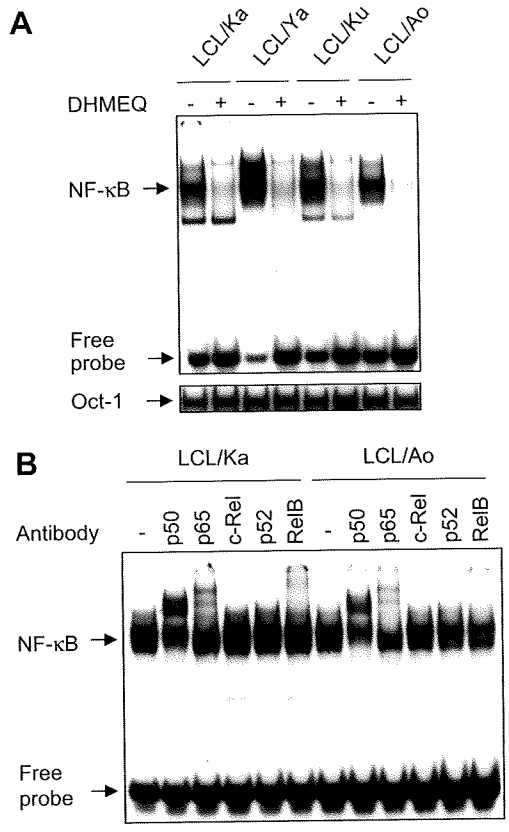

Fig. 1. Inhibition of constitutive NF-κB binding activity in LCLs by DHMEQ. (A) Inhibition of constitutive NF-κB activity in LCLs. LCLs were treated with 10 μg/ml of DHMEQ (+) or with DMSO alone (−) for 3 h. Nuclear extracts (2.5 μg) were examined for NF-κB binding activity by electrophoretic mobility shift analysis (EMSA) with a radiolabeled NF-κB-specific probe. Binding of Oct-1 served as a control. (B) Subcomponents of constitutive NF-κB activity in LCLs. Nuclear extracts (1 μg) of cells without DHMEQ treatment were subjected to supershift analysis with antibodies specific for NF-κB p50, p65, c-Rel, p52, and RelB or without antibody (−). The experiment using isotype matched IgG control showed the same result (data not shown). The position of shifted bands corresponding to NF-κB and free probes are indicated on the left.

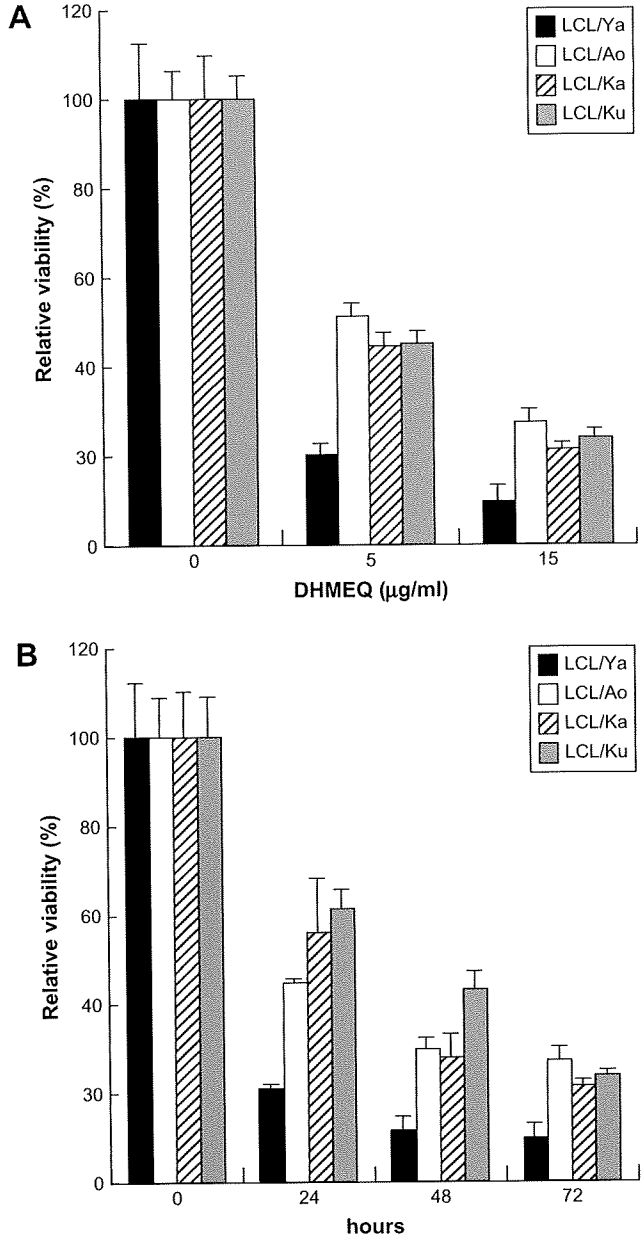

Fig. 2. DHMEQ inhibits proliferation of LCLs. The viability of the cells was determined by WST-8 assay and the relative levels compared with those of DMSO-treated cells are presented. Data represent the mean and standard deviation of triplicate experiments. (A) Results of dose–response experiments. LCLs were treated with 0, 5, or 10 μg/ml of DHMEQ for 72 h. ALL LCLs treated with 0, 5, or 10 μg/ml of DHMEQ showed statistical significance compared to DMSO-treated controls. (B) Results of time–response experiments. LCLs were treated with 10 μg/ml of DHMEQ for 24, 48, and 72 h. ALL LCLs treated for 24, 48, and 72 h except for LCL/Ku at the point of 24 h showed statistical significance compared to DMSO-treated controls.

Committee of the National Institute of Infectious Diseases approved the experimental protocol. 1×10^6 LCL cells were inoculated subcutaneously into the post-auricular region of NOG mice. DHMEQ was administered three times a week for 1 month into the post-auricular region of mice at a dose of 12 mg/kg, beginning on day 5 when tumors were palpable. The control mice were injected RPMI-1640 as was performed in our recent published papers [15,16]. Mice were killed 1 month after inoculation.

2.7. Immunohistochemistry

Cells were immunostained with antibodies and fluorescence signals were detected using confocal microscopy. Cytospin samples were prepared using 5×10^5 cells and cells were first washed three times with phosphate-buffered saline (PBS). Cells were then fixed with 100% cold acetone for 10 min at room temperature and washed three times in PBS. Samples were incubated with primary antibody at the concentration

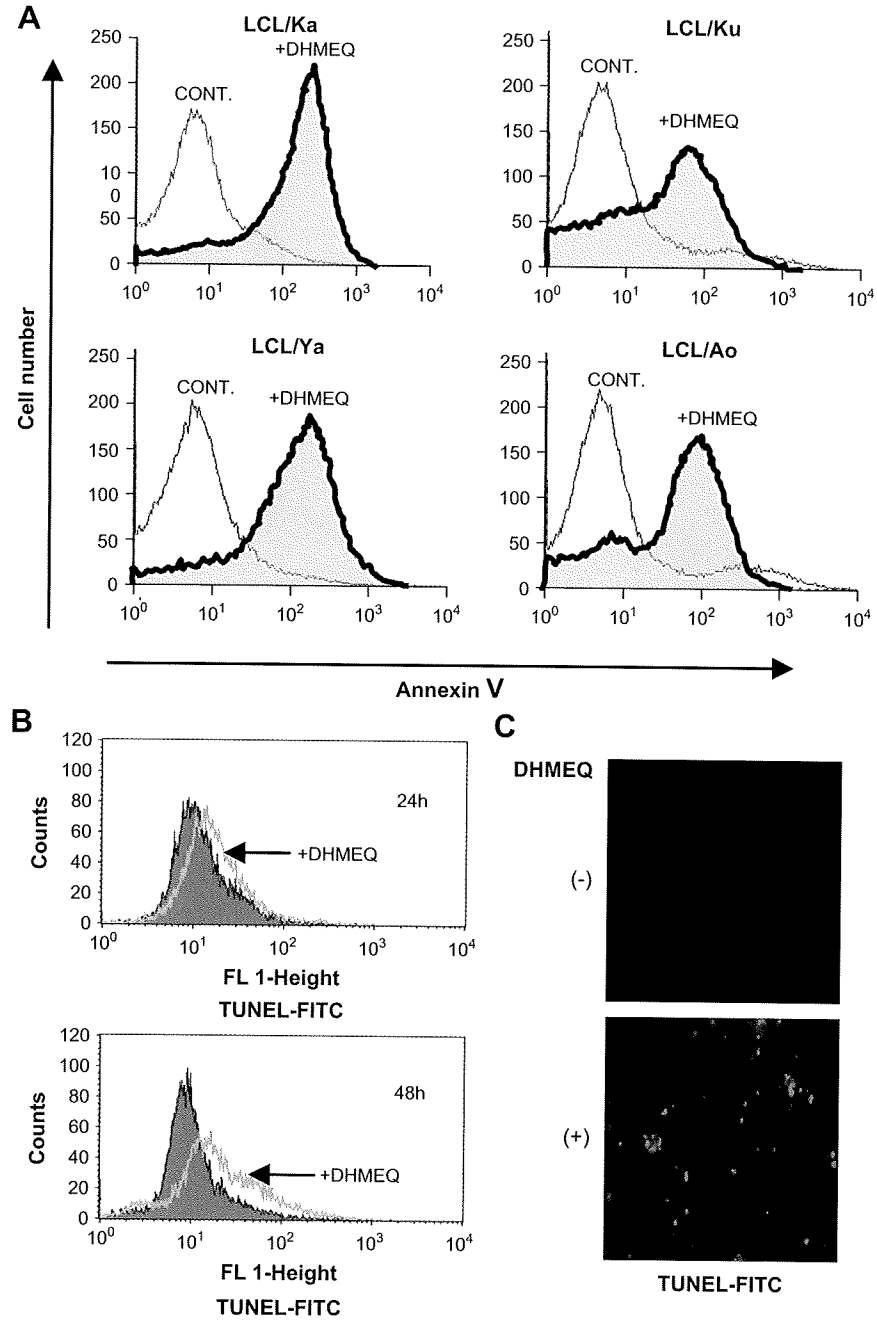

Fig. 3. DHMEQ induces apoptosis in LCLs. (A) Annexin V reactivity in LCLs after DHMEQ treatment. LCLs were treated with (filled curve) or without (open curve) 10 μg/ml of DHMEQ for 48 h, and the binding of FITC-conjugated Annexin V was analyzed by flow cytometry. (B) DNA fragmentation in LCL cells after DHMEQ treatment. DNA fragmentation in LCL cells was detected by TUNEL assay with flow cytometry. Representative flow cytometric profiles are shown for cells treated with 10 μg/ml of DHMEQ (open curve) or with DMSO alone (filled curve) for 24 h (upper panel) or 48 h (lower panel). (C) LCL cells were treated with 10 μg/ml of DHMEQ (+) or with DMSO alone (−) for 48 h, fixed on slides, and processed for TUNEL assay. A filter that selectively detects fluorescein isothiocyanate (FITC)-TUNEL fluorescence was used for the microscopic observation.

of 5 μg/ml at 4 °C overnight and washed with PBS three times. After incubation with fluorescence-labeled secondary antibody for 30 min at 37 °C, samples were washed three times in PBS and covered with a Perma Fluoro antifade reagent (Therme Shandon Co., Pittsburgh, PA). Fluorescence signals were detected using confocal microscopy (Radiance 2000) (Bio-Rad Laboratories. Antibodies used were as follows: anti-Epstein–Barr virus LMP clones CS, 1-4 mouse monoclonal antibody (Dako, Kyoto, Japan), and anti-p65 (c-20) goat polyclonal antibody (Santa Cruz Biotechnology Inc.

2.8. Real-time quantitative PCR

The expression level of anti-apoptotic genes was quantified by real-time reverse transcription–polymerase chain reaction (RT–PCR). Total RNA was extracted from the cells by ISOGEN reagent (Nippon Gene Co., Toyama, Japan) and treated according to the manufacturer's instructions. cDNA was synthesized using oligo dT and random primers synthesized with a PrimeScript RT reagent kit (Takara Bio Inc., Shiga, Japan). Amplification was performed with SYBR premix Ex Taq (Takara Bio Inc.) and the primer sets for c-IAP1, Bfl-1, BCL-XL, and c-FLIP (Takara Bio Inc.). The viral DNA load in EBV-infected PBMC was determined by real-time PCR with slight modifications of a previously described method [17]. DNA samples were extracted from the cells with a DNeasy tissue kit (Qiagen, Hilden, Germany). Amplification with SYBR premix Ex Taq (Takara Bio Inc.) and primers for BALF5 gene encoding the viral DNA polymerase (5′-CGG AAG CCC TCT GGA CTT C-3′ and 5′-CCC TGT TTA TCC GAT GGA ATG-3′) was performed using the Thermal Cycler Dice Real Time System (Takara Bio Inc.) and analyzed using the manufacturer's software.

2.9. Statistical analysis

Differences between mean values were assessed by *t*-test. A *P*-value of <0.05 was considered to be statistically significant.

3. Results

3.1. DHMEQ efficiently blocks constitutive NF-κB activity in LCLs

We first examined the effects of DHMEQ against constitutive NF-κB activity in established LCLs. Treatment with DHMEQ at a concentration of 10 μg/ml abrogated constitutive NF-κB binding activity in these cell lines (Fig. 1A). Components of NF-κB that are constitutively activated in LCLs were analyzed by

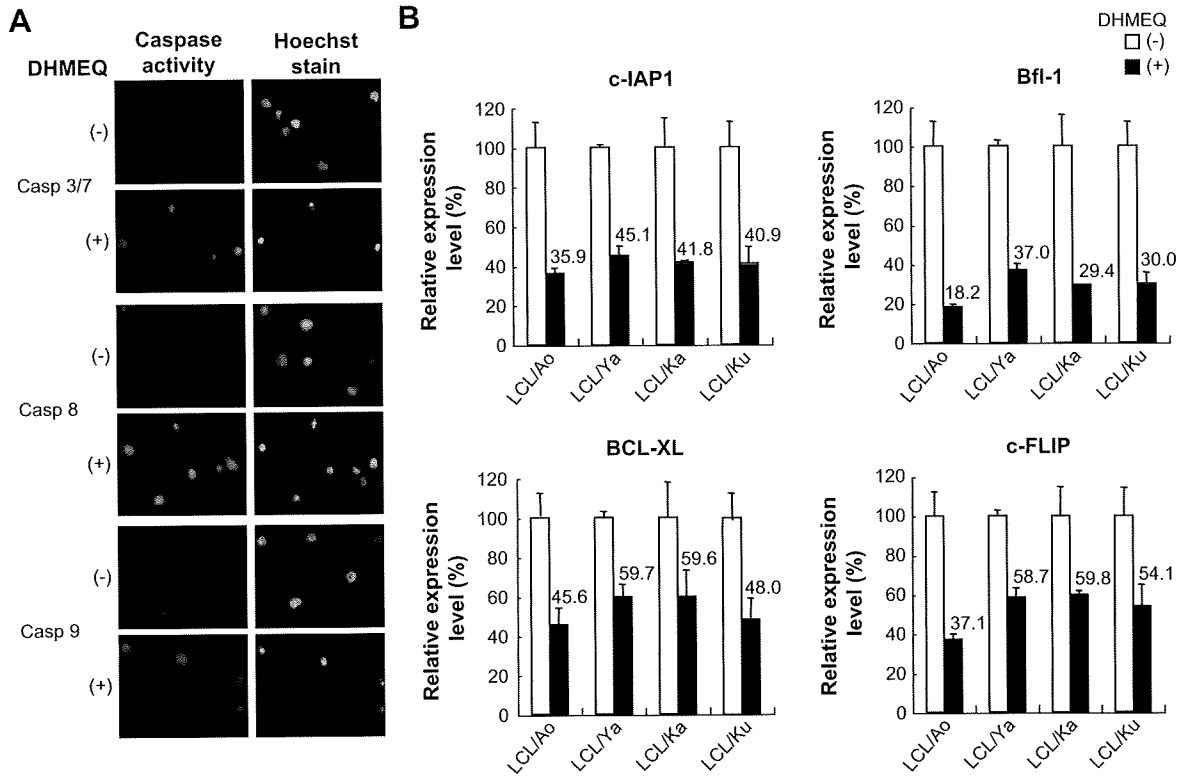

Fig. 4. Activation of caspase-3, -8, and -9. (A) LCL cells were treated with 10 μg/ml of DHMEQ (+) or with DMSO alone (−) for 8 h and fixed on slides. Caspase-3/7, -8, and -9 activities in LCLs after DHMEQ treatment were detected by green fluorochrome-labeled inhibitors of caspases (FLICA)-3/7, -8, and -9 (left panels) and nuclear DNA was stained with Hoechst 33342 (right panels). (B) Effects of DHMEQ on genes regulating apoptosis in LCLs. Quantification of the gene expression by real-time PCR. LCLs were treated with 10 μg/ml of DHMEQ (+) or with DMSO alone (−) for 4 h. The expressions of c-IAP1, Bfl-1, BCL-XL, and c-FLIP were quantified by real-time PCR. The data are means with standard deviation of triplicate experiments. The numbers above the bar graphs indicate the means of each gene expression after DHMEQ treatment. The reduction of the expressions of c-IAP1, Bfl-1, BCL-XL, and c-FLIP was statistically significant.

supershift assays. The results revealed that the NF-κB components consist of p50, p65, and RelB (Fig. 1B).

3.2. DHMEQ induces apoptosis of LCLs

To study the significance of NF-κB activation in the growth of LCLs, we examined the effects of DHMEQ on cell viability. Results of WST-8 assays showed that DHMEQ treatment reduced the cell viability of all four LCLs in a dose- and time-dependent manner (Fig. 2A and B).

NF-κB plays a key role in resistance to apoptosis [18]. Thus, we next examined whether DHMEQ induces apoptosis of LCLs by analyzing Annexin V reactivity and DNA fragmentation. Flow cytometric analysis showed a significant increase in the number of Annexin V-positive cells after DHMEQ treatment (Fig. 3A). Fragmentation of the nuclei of LCLs was clearly demonstrated after DHMEQ treatment by the TUNEL assay (Fig. 3B and C).

3.3. DHMEQ-induced apoptosis involves activation of caspases 3, 8, and 9

To confirm that the induction of apoptosis in LCLs by DHMEQ is caused by activation of the caspase pathway, we first examined activation of caspase-3/7 by immunostaining, using an antibody that recognizes a cleaved form of caspase-3/7. Results clearly showed cleavage of caspase-3/7, confirming that DHMEQ-induced apoptosis is associated with activation of the caspase pathway (Fig. 4A, top). To differentiate the membranous and mitochondrial pathways, we next examined the activation of caspases 8 and 9, which are upstream of caspase-3/7, by immunostaining. DHMEQ-treated LCL cells showed activation of both caspase-8 and caspase-9 (Fig. 4A, middle and bottom).

To understand the molecular mechanisms of apoptosis induction of LCLs after NF-κB inhibition by DHMEQ, we next examined by quantitative RT–PCR the changes in the expression levels of anti-apoptotic genes c-IAP1, Bfl-1, Bcl-XL, and c-FLIP, reportedly under the control of NF-κB, after DHMEQ treatment. The results demonstrated down-regulation of all of these genes (Fig. 4B).

3.4. DHMEQ shows a potent inhibitory effect on the growth of LCL cells in NOG mice

Because results *in vitro* suggested potential efficacy of DHMEQ for the treatment of patients with EBV-associated lymphoproliferative diseases, we next examined whether DHMEQ treatment can suppress the growth of xenografted LCL cells in a NOG mouse model. The gross appearance of resected tumors in mice treated with DHMEQ showed reduction of the tumor mass 1 month after inoculation of LCL cells (Fig. 5A and B). A decrease in the size of tumors in mice treated with DHMEQ was demonstrated when compared with controls 1 month after the injection of LCL cells (Fig. 5C).

3.5. DHMEQ inhibits outgrowth of EBV-infected peripheral blood B-lymphocytes

EBV-infected B lymphocytes under immunocompromised conditions acquire latency III infection, which may lead to proliferation and transformation into lymphoproliferative diseases including lymphomas [2,3]. Previous data link NF-κB activation by LMP-1 to transformation; however, they also indicate that NF-κB activation is not sufficient for transformation and should coordinate with other signals like mitogen-activated protein kinases [19]. Roles of NF-κB activity in EBV-infected lymphocytes for their survival during the early phase of infection are not fully understood. Therefore, to investigate the roles of NF-κB activation on the survival of EBV-infected lymphocytes during the early phase of infection, we examined the effect of NF-κB inhibition by DHMEQ on their survival and the EBV viral load in PBMC infected with EBV. Lymphocytes infected with EBV under immunosuppressive conditions already show constitutive NF-κB activation as well as LMP1 expression. Treatment of these cells with DHMEQ inhibited translocation of NF-κB into the nucleus (Fig. 6A). DHMEQ treatment also eliminated LMP1-expressing lymphocytes from PBMC (Fig. 6B). Finally, DHMEQ treatment prevented the outgrowth of lymphocytes infected

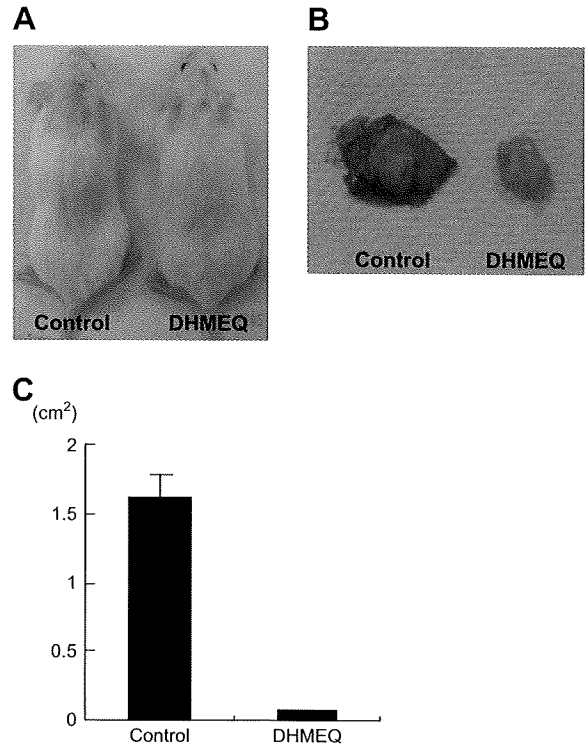

Fig. 5. DHMEQ inhibited the tumor growth of LCL cells *in vivo*. NOG mice were inoculated with LCL cells and administered DHMEQ (12 mg/kg) ($n = 5$) or control medium ($n = 5$) subcutaneously in the post-auricular region three times a week for up to 1 month. (A) Photograph of the backs of mice. (B) Photograph of a tumor at the site of LCL cells inoculation. (C) Subcutaneous tumor volume of mice inoculated with LCL cells and administered DHMEQ or control medium 1 month after inoculation.

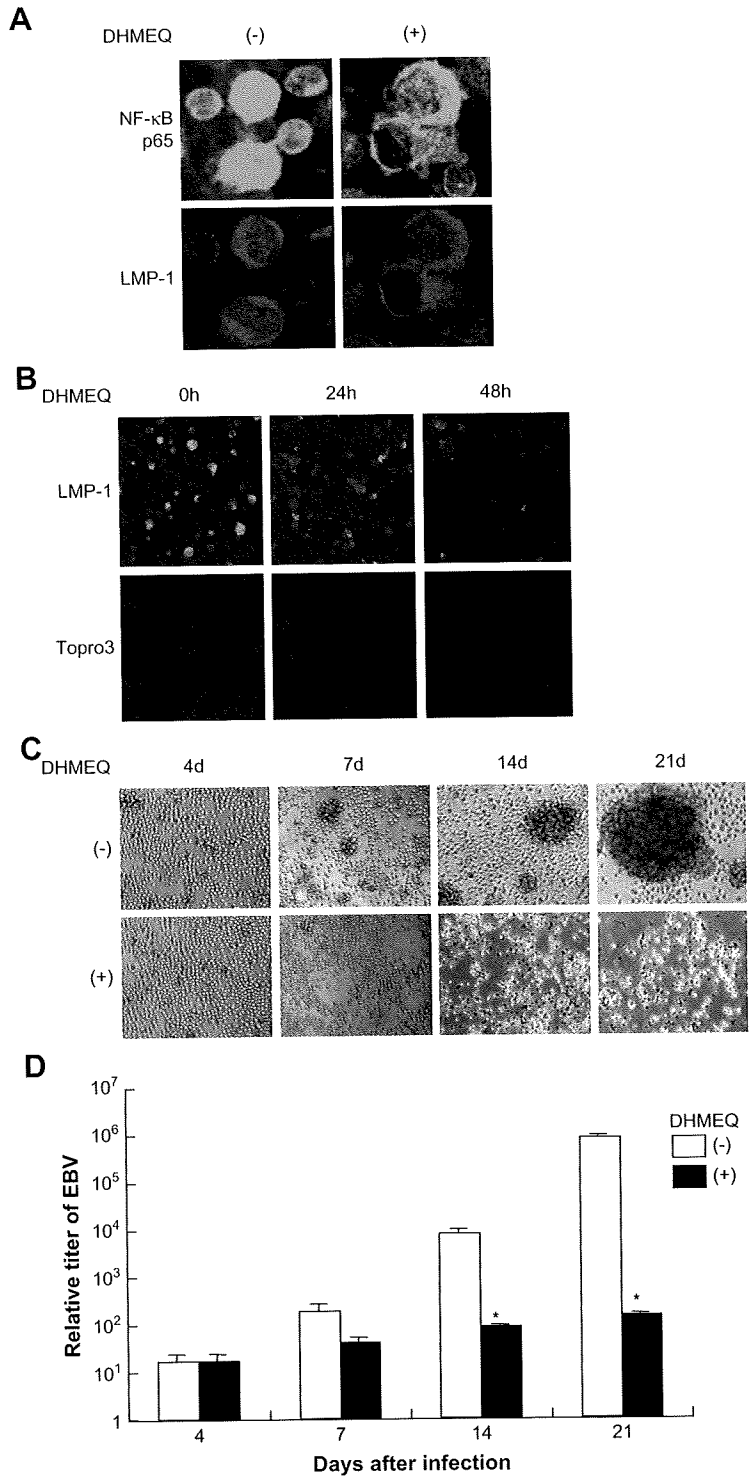

Fig. 6. Effects of DHMEQ on PBMC infected with EBV. 8×10^5/ml of PBMC from a healthy donor infected with EBV using supernatant of B95.8 line were cultured in RPMI 1640 medium supplemented with 10% FBS and 200 ng/ml cyclosporine A. Cells were harvested 4 days and 14 days after infection and served for experiments. (A) Inhibition of NF-κB and expression of LMP1 in lymphocytes. At the point of 4 days after infection, cells were treated with or without 10 μg/ml of DHMEQ for 1 h and immunostained with antibodies for LMP1 and NF-κB p65. DMSO-treated cells served as a control. (B) DHMEQ treatment eliminated LMP1 expressing cells from PBMC. At the point of 14 days after infection, cells were treated with or without 10 μg/ml DHMEQ for the indicated number of hours. Cells stained with anti-LMP1 antibody and topro 3 were observed by confocal microscopy. DMSO-treated cells served as a control. (C, D) Photographs of EBV-infected PBMC and quantification of viral load by real-time PCR. Cells cultured for 4 days were treated with 10 μg/ml of DHMEQ (+) or with DMSO alone (−) thereafter twice a week. Cells were observed by microscopy at the indicated days (C). Cells were harvested on the indicated days and genomic DNA was isolated. The viral load was quantified by real-time PCR as described in Section 2. The data are means and standard deviations of triplicate experiments (D). The asterisks indicate statistical significance.

with EBV and decreased the EBV viral load in PBMC (Fig. 6C and D).

4. Discussion

In the present study, we showed that the NF-κB inhibitor DHMEQ blocked strong and constitutive NF-κB activity, reduced viability, and induced apoptosis in LCLs. Induction of apoptosis by DHMEQ in LCLs is associated with inhibition of NF-κB, which is followed by down-regulation of NF-κB regulated anti-apoptotic genes. These observations, combined with our previous study about the mechanisms of action of DHMEQ [11], indicate that apoptosis induction of LCLs by DHMEQ is mediated by inhibitory effect of DHMEQ against NF-κB. DHMEQ appears to be more specific to NF-κB pathway compared with IκB kinase (IKK) inhibitor, Bay 11-7082 used in the previous studies [20,21], because DHMEQ inhibits downstream of IKK and Bay 11-7082 has been reported to be apparently not specific for NF-κB pathway [22]. Therefore our study provides further evidence for the importance of NF-κB in the survival of LCLs and indicates effectiveness of DHMEQ in the treatment of EBV-infected transformed lymphocytes.

We also showed that DHMEQ inhibits constitutive NF-κB activation in B lymphocytes expressing LMP1, eliminates these cells from PBMC, and inhibits the outgrowth of lymphoblastic cells. The results indicate that B lymphocytes become dependent on NF-κB for proliferation and survival within several days after EBV infection. Although previous data indicate that not only NF-κB but also other signals like mitogen-activated protein kinases are involved in transformation of lymphocytes to LCL cells [19], the results in this study indicates that abrogation of constitutive NF-κB activity appears to be sufficient to prevent transformation of EBV-infected lymphocytes. Previous reports underscored constitutive NF-κB activity as a molecular target in LCL cells [20,21,23]. Our study shows a new insight that constitutive NF-κB activity is a common molecular target in EBV-infected transformed and untransformed lymphocytes.

Recent reports showed that EBV viral load is a useful marker for disease status of lymphoproliferative diseases or lymphomas in patients with immunosuppression [24]. We showed that DHMEQ treatment prevented the increase of EBV viral load in PBMC. The reduction of EBV viral load in PBMC by DHMEQ indicates not only that the elimination of lymphocytes infected by EBV contributes to the reduction, but also that the replication of EBV virus may depend on NF-κB activity. However, previous studies showed that NF-κB activity does not promote replication of EBV virus, but rather inhibits its replication [25]. Therefore, reduction of viral load in lymphocytes infected with EBV treated with DHMEQ appears to be due to the elimination of lymphocytes infected with EBV. Collectively, early detection of the increase of EBV viral load and purging infected cells under transformation by a NF-κB inhibitor may contribute to the preventive intervention against lymphoproliferative diseases in patients with profound immunosuppression.

Our results suggest that the effects of DHMEQ depend on the down-regulation of NF-κB-dependent genes that control apoptosis. Down-regulation of c-FLIP, involved in anti-apoptosis blocking caspase-8, as well as Bfl-1, Bcl-XL and c-IAP, involved in the anti-apoptosis blocking caspase-9, by DHMEQ may result in activation of membranous and mitochondrial pathways, respectively [26]. This implies the possibility that in EBV-infected lymphocytes, the induction of anti-apoptotic genes is counteracting the apoptotic pressure and preventing these cells from undergoing apoptosis.

The mice treated with DHMEQ in 1% DMSO did not show any relevant signs of toxicity such as body weight loss in this experiment. The dose of DHMEQ administered in this experiment was 12 mg/kg three times a week, far less than the LD_{50} of DHMEQ, 180 mg/kg (Naoki Matsumoto, K.U., unpublished observation, July 1999). Results of our in vivo model suggest that DHMEQ may be feasible and less toxic at an effective dose, although the pharmacokinetics has not yet been elucidated. In our NOG mice model, the results indicate that local administration of DHMEQ can prevent primary tumor growth without significant signs of toxicity. Additional experiments, which include intraperitoneal and intravenous administration of DHMEQ, will further confirm efficacy of DHMEQ against LCLs *in vivo*.

Our recent study also indicates that DHMEQ has little effect on the viability of PBMC or purified B cells *in vitro* under almost the same experimental condition as this study [27]. These *in vitro* and *in vivo* results suggest a favorable toxic profile and potent NF-κB inhibitory effect by DHMEQ. Thus, DHMEQ appears to be a candidate for the treatment of EBV-associated lymphoproliferative diseases as well as for their chemoprevention.

In conclusion, our study indicates that the unique NF-κB inhibitor DHMEQ is a potential compound that targets constitutive activation of NF-κB in EBV-infected transformed and untransformed B cells. Because EBV-associated lymphoproliferative diseases are life-threatening and the prognosis of AIDS-associated lymphomas is extremely unfavorable, our results support preventive intervention with a NF-κB inhibitor as a new strategy in patients with immunosuppression.

Acknowledgments

This work was supported in part by Grants-in-Aid for Scientific Research from the Japan Society for Promotion of Science (R.H. and T.W.). This work was also supported by grants from the Japanese Ministries of Education, Culture, Sport Science and Technology and Health, Labour and Welfare, as well as the Human Health Science of Japan (N.Y.).

References

[1] J.I. Cohen, Epstein–Barr virus infection, N. Engl. J. Med 343 (2000) 481–492.
[2] K.F. Macsween, D.H. Crawford, Epstein–Barr virus-recent advances, Lancet Infect. Dis 3 (2003) 131–140.
[3] E. Klein, L.L. Kis, G. Klein, Epstein–Barr virus infection in humans: from harmless to life endangering virus-lymphocyte interactions, Oncogene 26 (2007) 1297–1305.

[4] S. Gottschalk, C.M. Rooney, H.E. Heslop, Post-transplant lymphoproliferative disorders, Annu. Rev. Med 56 (2005) 29–44.
[5] C. Diamond, T.H. Taylor, T. Aboumrad, H. Anton-Culver, Changes in acquired immunodeficiency syndrome-related non-Hodgkin lymphoma in the era of highly active antiretroviral therapy: incidence, presentation, treatment, and survival, Cancer 106 (2006) 128–135.
[6] Y. Hoshida, J.X. Xu, S. Fujita, I. Nakamichi, J. Ikeda, Y. Tomita, S. Nakatsuka, J. Tamaru, A. Iizuka, T. Takeuchi, K. Aozasa, Lymphoproliferative disorders in rheumatoid arthritis: clinicopathological analysis of 76 cases in relation to methotrexate medication, J. Rheumatol 34 (2007) 322–331.
[7] D.C. Guttridge, C. Albanese, J.Y. Reuther, R.G. Pestell, A.S. Baldwin Jr., NF-kappaB controls cell growth and differentiation through transcriptional regulation of cyclin D1, Mol. Cell. Biol. 19 (1999) 5785–5799.
[8] O. Devergne, E. Hatzivassiliou, K.M. Izumi, K.M. Kaye, M.F. Kleijnen, E. Kieff, G. Mosialos, Association of TRAF1, TRAF2, and TRAF3 with an Epstein–Barr virus LMP1 domain important for B-lymphocyte transformation: role in NF-kappaB activation, Mol. Cell. Biol. 16 (1996) 7098–7108.
[9] T.D. Gilmore, Introduction to NF-kappaB: players, pathways, perspectives, Oncogene 25 (2006) 6680–6684.
[10] N. Matsumoto, A. Ariga, S. To-e, H. Nakamura, N. Agata, S. Hirano, J. Inoue, K. Umezawa, Synthesis of NF-kappaB activation inhibitors derived from epoxyquinomicin C, Bioorg. Med. Chem. Lett. 10 (2000) 865–869.
[11] A. Ariga, J. Namekawa, N. Matsumoto, J. Inoue, K. Umezawa, Inhibition of tumor necrosis factor-alpha-induced nuclear translocation and activation of NF-kappa B by dehydroxymethylepoxyquinomicin, J. Biol. Chem. 277 (2002) 24625–24630.
[12] G. Miller, M. Lipman, Comparison of the yield of infectious virus from clones of human and simian lymphoblastoid lines transformed by Epstein–Barr virus, J. Exp. Med 138 (1973) 1398–1412.
[13] N.C. Andrews, D.V. Faller, A rapid micropreparation technique for extraction of DNA-binding proteins from limiting numbers of mammalian cells, Nucleic Acids Res. 19 (1991) 2499.
[14] J. Inoue, L.D. Kerr, L.J. Ransone, E. Bengal, T. Hunter, I.M. Verma, c-rel activates but v-rel suppresses transcription from kappa B sites, Proc. Natl. Acad. Sci. USA 88 (1991) 3715–3719.
[15] M.Z. Dewan, J.N. Uchihara, K. Terashima, M. Honda, T. Sata, M. Ito, N. Fujii, K. Uozumi, K. Tsukasaki, M. Tomonaga, Y. Kubuki, A. Okayama, M. Toi, N. Mori, N. Yamamoto, Efficient intervention of growth and infiltration of primary adult T-cell leukemia cells by an HIV protease inhibitor, ritonavir, Blood 107 (2006) 716–724.
[16] M. Watanabe, M.Z. Dewan, T. Okamura, M. Sasaki, K. Itoh, M. Higashihara, H. Mizoguchi, M. Honda, T. Sata, T. Watanabe, N. Yamamoto, K. Umezawa, R. Horie, A novel NF-kappaB inhibitor DHMEQ selectively targets constitutive NF-kappaB activity and induces apoptosis of multiple myeloma cells in vitro and in vivo, Int. J. Cancer 114 (2005) 32–38.
[17] H. Kimura, M. Morita, Y. Yabuta, K. Kuzushima, K. Kato, S. Kojima, T. Matsuyama, T. Morishima, Quantitative analysis of Epstein–Barr virus load by using a real-time PCR assay, J. Clin. Microbiol. 37 (1999) 132–136.
[18] J. Dutta, Y. Fan, N. Gupta, G. Fan, C. Gelinas, Current insights into the regulation of programmed cell death by NF-kappaB, Oncogene 25 (2006) 6800–6816.
[19] E.D. Cahir McFarland, K.M. Izumi, G. Mosialos, Epstein–Barr virus transformation: involvement of latent membrane protein 1-mediated activation of NF-kappaB, Oncogene 18 (1999) 6959–6964.
[20] E.D. Cahir-McFarland, K. Carter, A. Rosenwald, J.M. Giltnane, S.E. Henrickson, L.M. Staudt, E. Kieff, Role of NF-kappa B in cell survival and transcription of latent membrane protein 1-expressing or Epstein–Barr virus latency III-infected cells, J. Virol 78 (2004) 4108–4119.
[21] S.A. Keller, D. Hernandez-Hopkins, J. Vider, V. Ponomarev, E. Hyjek, E.J. Schattner, E. Cesarman, NF-kappaB is essential for the progression of KSHV- and EBV-infected lymphomas in vivo, Blood 107 (2006) 3295–3302.
[22] J.W. Pierce, R. Schoenleber, G. Jesmok, J. Best, S.A. Moore, T. Collins, M.E. Gerritsen, Novel inhibitors of cytokine-induced IkappaBalpha phosphorylation and endothelial cell adhesion molecule expression show anti-inflammatory effects in vivo, J. Biol. Chem. 272 (1997) 21096–21103.
[23] E.D. Cahir-McFarland, D.M. Davidson, S.L. Schauer, J. Duong, E. Kieff, NF-kappa B inhibition causes spontaneous apoptosis in Epstein–Barr virus-transformed lymphoblastoid cells, Proc. Natl. Acad. Sci. USA 97 (2000) 6055–6060.
[24] S.M. Aalto, E. Juvonen, J. Tarkkanen, L. Volin, T. Ruutu, P.S. Mattila, H. Piiparinen, S. Knuutila, K. Hedman, Lymphoproliferative disease after allogeneic stem cell transplantation–pre-emptive diagnosis by quantification of Epstein–Barr virus DNA in serum, J. Clin. Virol 28 (2003) 275–283.
[25] H.J. Brown, M.J. Song, H. Deng, T.T. Wu, G. Cheng, R. Sun, NF-kappaB inhibits gammaherpesvirus lytic replication, J. Virol 77 (2003) 8532–8540.
[26] J.M. Adams, Ways of dying: multiple pathways to apoptosis, In: Genes Dev, 17 (2003) 2481–2495.
[27] R. Horie, M. Watanabe, T. Okamura, M. Taira, M. Shoda, T. Motoji, A. Utsunomiya, T. Watanabe, M. Higashihara, K. Umezawa, DHMEQ, a new NF-kappaB inhibitor, induces apoptosis and enhances fludarabine effects on chronic lymphocytic leukemia cells, Leukemia 20 (2006) 800–806.

Transient inhibition of NF-κB by DHMEQ induces cell death of primary effusion lymphoma without HHV-8 reactivation

Nazanin Dabaghmanesh,[1] Aiko Matsubara,[1,2] Ariko Miyake,[1] Kazumi Nakano,[1] Takaomi Ishida,[1] Harutaka Katano,[3] Ryoichi Horie,[4] Kazuo Umezawa[5] and Toshiki Watanabe[1,6]

[1]Department of Medical Genome Sciences, Graduate School of Frontier Sciences, The University of Tokyo, 4-6-1 Shirokanedai, Minato-ku, Tokyo 108-8639, Japan; [2]Faculty of Medicine, The University of Tokyo, 7-3-1 Hongo, Bunkyo-ku, Tokyo 113-0033, Japan; [3]Department of Pathology, National Institute of Infectious Diseases, 1-23-1 Toyama, Shinjyuku-ku, Tokyo 162-8640, Japan; [4]Department of Hematology, Faculty of Medicine, Kitasato University, 1-15-1 Kitasato, Sagamihara-shi, Kanagawa 228-8555, Japan; [5]Department of Applied Chemistry, Faulty of Science and Technology, Keio University, 3-14-1 Hiyoshi, Kohoku-ku, Yokohama-shi, Kanagawa 223-8522, Japan

(Received July 5, 2008/Revised November 7, 2008/Accepted December 3, 2008/Online publication February 17, 2009)

Primary effusion lymphoma (PEL) is a refractory malignancy caused by human herpes virus 8 (HHV-8) in immunocompromised individuals. The tumor cells of PEL are characterized by constitutive NF-κB activation. Dehydroxymethylepoxyquinomicin (DHMEQ) is a new NF-κB inhibitor and is effective on various tumor cells with constitutively activated NF-κB. Thus, in search for a new therapeutic modality of PEL, we examined the effect of DHMEQ on PEL cells. We confirmed constitutive activation of NF-κB with subcomponents of p50 and p65 in PEL cell lines. DHMEQ quickly and transiently abrogated NF-κB activation and reduced the cell viability in dose- and time-dependent manners, inducing apoptosis through activation of both mitochondrial and membrane pathways. Array analysis revealed that DHMEQ down-regulated expression levels of NF-κB target genes, such as *interleukin-6* (IL6), *Myc*, chemokine (C-C motif) receptor 5 (*CCR5*) and NF-κB1, whereas it up-regulated expression levels of some genes involved in apoptosis, and cell cycle arrest. DHMEQ did not reactivate HHV-8 lytic genes, indicating that NF-κB inhibition by DHMEQ did not induce virus replication. DHEMQ rescued CB-17 SCID mice xenografted with PEL cells, reducing the gross appearance of effusion. Thus, DHMEQ transiently abrogated the NF-κB activation, irreversibly triggering the apoptosis cascade without HHV-8 reactivation. In addition, DHMEQ could rescue the PEL-xenograft mice. Therefore, we suggest DHMEQ as a promising candidate for molecular target therapy of the PEL. (*Cancer Sci* 2009; 100: 737–746)

Primary effusion lymphoma (PEL) is a non-Hodgkin B-cell lymphoma usually associated with immunocompromised patients such as those with aquired immune defficiency syndrome (AIDS).[1,2] Despite extensive use of highly active antiretroviral treatment (HAART) and improvement of chemotherapy management in human immunodeficiency virus (HIV)-infected patients, the prognosis of patients with HIV-related PEL remains poor. The median survival does not exceed 6 months even in the most recent series.[3] The tumor cells have an intermediate immunophenotype but B-cell genotyping shows clonal rearrangements of immunoglobulin genes.[4]

Human herpes virus 8 (HHV-8) is essential for the development of PEL that is universally associated with HHV-8. Most of the PELs are also infected with Epstein–Barr virus (EBV) and the combination of the two viruses might promote full transformation. Tumor cells in PELs are latently infected by HHV-8 and express latent proteins, while a few cells undergo lytic replication. HHV-8 encodes numerous proteins homologous to critical cell cycle regulatory and apoptosis proteins, cellular receptors and their ligands. However, because of their unique properties they can escape normal regulatory pathways and hence behave differently from their cellular counterparts. Among these genes, v-cyclin, LANA, and v-IRF1 interfere with the cell cycle deregulation, while v-FLIP prevents apoptosis.[5] PELs have constitutively active nuclear factor (NF)-κB, due to v-FLIP expression, which is essential for their survival.[6–10] In addition to v-FLIP, HHV-8 proteins K1, K15, and the viral G protein-coupled receptor (v-GPCR) induce NF-κB activity, thereby supporting the central role of NF-κB signaling in HHV-8 pathogenesis.[5]

NF-κB has been implicated in inflammation, cell proliferation, differentiation, apoptosis and cell survival. NF-κB is a ubiquitously expressed family of five proteins; p65 (RelA), p50, p52, c-Rel and RelB. Different combinations of these NF-κB subunits are considered to specify target genes under different conditions.[11,12]

Dehydroxymethylepoxyquinomicin (DHMEQ) is an NF-κB inhibitor, based on the structure of antibiotic epoxyquinomicin C.[13] DHMEQ inhibits the tumor necrosis factor (TNF)-α-induced NF-κB binding activity but not the phosphorylation or degradation of I-κB. DHMEQ inhibited the TNF-α-induced nuclear accumulation of p65. Thus, DHMEQ is a unique inhibitor of NF-κB that acts at the level of the nuclear translocation.[14] DHMEQ has been reported to be effective on various hematologic and solid malignancies with constitutively active NF-κB.[15–21]

Therefore, in search for a new modality of PEL therapy based on the idea of molecular targeting, we examined effects of DHMEQ on PEL cells *in vitro* and *in vivo*. Our data demonstrated that DHMEQ could abrogate the NF-κB activation transiently and initiate the apoptosis cascade irreversibly without activation of HHV-8 replication. In addition, DHMEQ rescued the PEL xenograft mice. Taken together, we suggest DHMEQ as a promising candidate for molecular target therapy of the PEL.

Materials and Methods

Cell culture. PEL cell lines used for experiments are BCBL1, TY1 and BC1 infected with HHV-8.[22,23] BC1 was also infected by EBV. Jurkat and K562 cells were obtained from the Japanese Cancer Research Resources Bank (Tokyo, Japan). These cell lines were cultured in RPMI 1640 medium (Gibco, Carlsbad, CA, USA) supplemented with 10% fetal bovine serum (FBS) (Bio West, Miami, FL, USA) and antibiotics (penicillin/streptomycin, Gibco), except for BC1 and TY1 cells that were cultured with 20% FBS.

[6]To whom correspondence should be addressed. E-mail: tnabe@ims.u-tokyo.ac.jp

doi: 10.1111/j.1349-7006.2009.01083.x

Table 1. Primers used in the real time quantitative reverse transcription–polymerase chain reaction

Gene		Sequence of oligonucleotide
DDIT3	sense	5′-GCCAAAATCAGAGCTGGAAC-3′
	antisense	5′-TCTTGCAGGTCCTCATACCA-3′
DEDD2	sense	5′-GCAGTCAAGCAGTTCTGCAA-3′
	antisense	5′-CACAGGTCACTTTGCCTTCA-3′
p21	sense	5′-GCAGACCAGCATGACAG-3′
	antisense	5′-TAGGGCTTCCTCTTGGA-3′
IL6	sense	5′-GGTACATCCTCGACGGCATCT-3′
	antisense	5′-GTGCCTCTTTGCTGCTTTCAC-3′
BIRC3	sense	5′-CAGCCCGCTTTAAAACATTC-3′
	antisense	5′-ACCCATGGATCATCTCCAG-3′
MYC	sense	5′-GCCACGTCTCCACACATCAG-3′
	antisense	5′-TCTTGGCAGCAGGATAGTCCTT-3′

Electrophoretic mobility shift assays (EMSAs) and supershift analysis. For detecting NF-κB binding, we used an NF-κB consensus oligonucleotide (Promega Corporation, Madison, WI, USA).[24] Nuclear extracts were prepared basically as described.[23] DNA-protein complexes were analyzed as previously described.[25] The supershift analysis was performed as described previously, using antibodies against p65, p50, p52, c-Rel, and Rel-B (all from Santa Cruz Biotechnology, Santa Cruz, CA, USA), or a control mouse immunoglobulin G.[26]

Assessment of cell viability and apoptosis. Cell viability was determined by color reaction with WST-8. Cell Counting Kit-8 (Dojindo, Kumamoto, Japan), and Annexin V reactivity was examined by Annexin V using Apopcyto Annexin V-Azami-Green Apoptosis detection kit (MBL, Nagoya, Japan) according to the manufacture's protocols. Terminal deoxynucleotidyl transferase-mediated dUTP nick-end labeling (TUNEL) assay was performed using DeadEnd Fluorometric TUNEL System (Promega Corporation) kit and protocols. The results for both tests were analyzed using FACSCalibur machine and CellQuest software (BD Biosciences, San Jose, CA, US). Cell cycle analysis was done as described previously,[15] at 6 h after DHMEQ treatment. The resulting DNA histograms were interpreted using the FlowJo (Tree Star Inc., Ashland, OR, US) combined with the Watson Pragmatic model.

Caspase activity detection. Activation of caspases-3, -8, and -9 were assessed by Carboxyfluorescein FLICA Apoptosis Detection Kit (Immunochemistry Technologies, Bloomington, MN, USA) according to the manufacturer's instructions. Cleavage of the caspases was confirmed by detection of cleaved products by immunoblot analysis using antibodies specific to cleaved products of caspase 3 and 9, or reactive to both cleaved and uncleaved caspase-8. The antibodies used are: cleaved caspase-3 (Asp175) antibody, caspase-8 (1C12) mouse mAb, and cleaved caspase-9 (Asp330) antibody (human-specific; all form Cell Signaling Technology, Beverly, MA, USA). Immunoblotting analysis was done basically as described previously.[18]

Microarray experiment. Total RNA was extracted from BC1 and BCBL1 cells treated with or without DHMEQ (10 μg/mL) for 6 h, using Trizol. Whole Human Genome Oligo Microarray Kit (Agilent Technologies, Santa Clara, CA, USA) was used to evaluate the gene expression in PEL cell lines according to the manufacturer's protocols. Whole data analyses were conducted using the software GeneSpring (Agilent Technologies). First, Student *t*-tests were performed in order to extract genes with expression levels significantly different between samples with and without DHMEQ treatment ($P < 0.01$). Secondly, gene ontology analyses were performed on that group of genes in BC1 in order to categorize the selected genes at the significant levels of $P < 0.01$.

Reverse transcription–polymerase chain reaction (RT-PCR) and real-time RT-PCR. Total RNA was extracted from the cells using the ISOGEN Kit (Wako Chemical Industry, Osaka, Japan). First-strand cDNAs were synthesized using 2 μg of the total RNA and 500 ng Oligo $(dT)_{12-18}$ using SuperScript™ II RT (Invitrogen Japan, Tokyo, Japan). RT-PCR was done for 25 cycles by Gene *Taq* enzyme (Wako Chemical Industries) with 10 pmoles of HHV-8 gene-specific primers. PCR products were analyzed by agarose gel electrophoresis and ethidium bromide staining. The primers for ORFK13 (*v-FLIP*), ORF72 (*v-cyclin*), ORF73 (*LANA*), ORF50 (*Rta*), ORFK9 (*v-IRF*) and ORF74 (*v-GPCR*) are the same as those used in the previous reports.[27–29]

For the real-time RT-PCR, cDNAs were synthesized by PrimeScript RT Reagent Kit (TAKARA Bio Inc., Shiga, Japan). PCR was performed with a SYBR Premix Ex*Taq* (TAKARA Bio Inc.) and the primer sets are listed in Table 1. Reactions were performed with a Thermal Cycler Dice Real Time System (TAKARA Bio Inc.) and analyzed using the manufacturer's software. For quantification, the expression levels of six genes were normalized with that of *GAPDH* gene.

***In vivo* therapeutic effect of DHMEQ.** Twenty male CB17 SCID mice were obtained from CLEA Japan Company. Mice at 5 weeks old were injected with 4×10^6 TY1 cells intraperitoneally. In the treatment group, DHMEQ dissolved in 0.5% carboxymethyl cellulose (CMC) (Sigma, St. Louis, MO, USA) solution was administered into the intraperitoneal region at a dose of 8 mg/kg, beginning 1 day before the inoculation and 3 times a week thereafter for 1 month. In the control group, mice were treated with dimethyl sulfoxide (DMSO) dissolved in 0.5% CMC solution by the same procedure. Mice were observed for 3 months and survival curves were calculated by Kaplan and Meier's method. The statistical significance was examined by Cox-Mantel test. A *P*-value < 0.05 was considered to be statistically significant.

Results

NF-κB activation was abrogated in PEL cell lines by DHMEQ. NF-κB is constitutively activated in primary PEL cells and cell lines derived from them.[9,30] Thus, we first confirmed NF-κB activation by EMSA and analyzed its subcomponents by supershift assays, using TY1, BCBL1 and BC1 cell lines. The results confirmed constitutive activation of NF-κB in BCBL1 and BC1 cell lines as previously reported,[9,30] and NF-κB activation was first confirmed in TY1 in this experiment. Supershift analyses showed that NF-κB bands were composed of p50, p65 and RelB in all cell lines, indicating constitutive activation of both canonical and non-canonical pathways. Furthermore, it was clearly demonstrated that the major NF-κB binding signals are composed of two bands, the lower one containing p50 and upper one p65 (Fig. 1A).

We next tested the effects of DHMEQ treatment of these cells. Results of EMSA demonstrated loss of DNA binding of NF-κB after 1–3 h. However, all cell lines showed significant recovery of NF-κB activities after short periods. TY1 and BCBL1 cells lost NF-κB binding activity at 1 h; however, recovery was evident at 3 or 6 h with almost full recovery at 24 h. BC1 cells recovered almost the initial level of NF-κB activity after 24 h (Fig. 1B). These results indicated that DHMEQ could transiently inhibit NF-κB activity in PEL cell lines with partial or full recovery of the activities in 1 day. In other lymphoid cell lines, recovery of NF-κB activity after DHMEQ treatment was not observed in 1 day,[16–18] although a weak binding of NF-κB could be detected sometimes at later time points (unpublished observation). Thus, relatively quick recovery of NF-κB activity appears to be a unique feature of PEL cell lines.

DHMEQ reduced cell viability in PEL cell lines. Next we examined the cell viability after 3 days incubation with different

doi: 10.1111/j.1349-7006.2009.01083.x

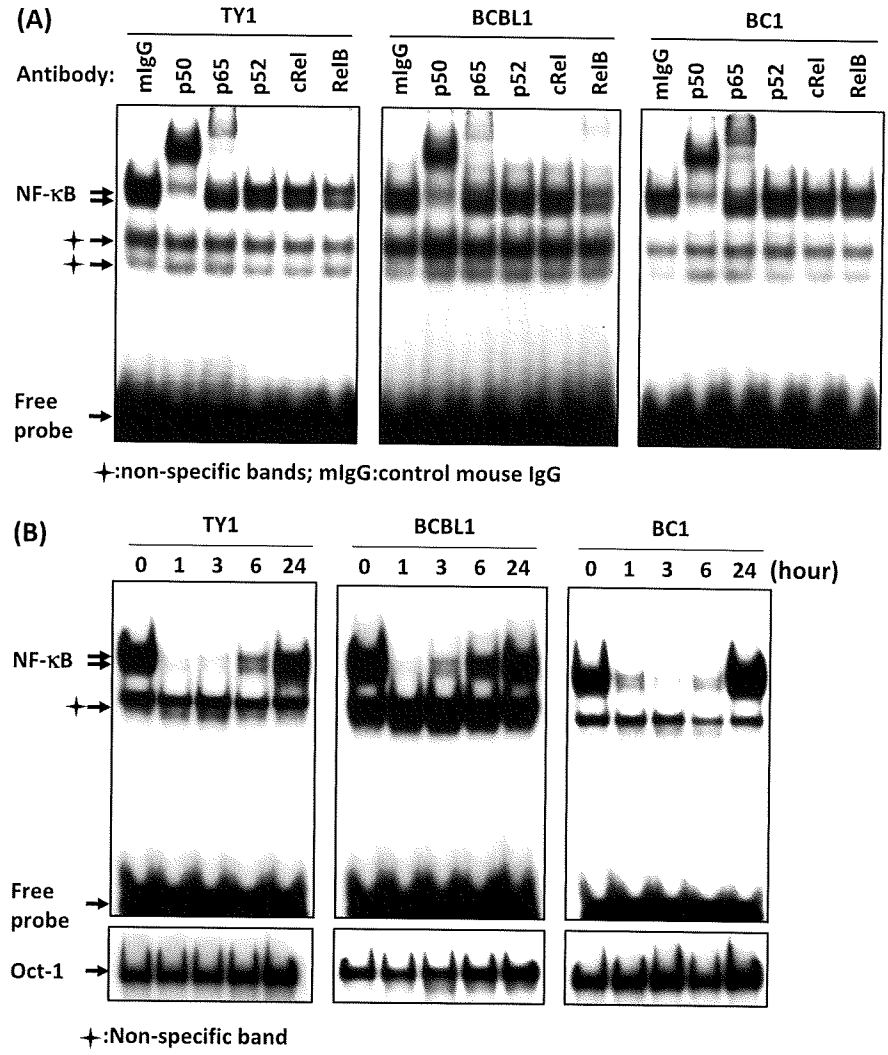

Fig. 1. Dehydroxymethylepoxyquinomicin (DHMEQ) inhibited constitutive NF-κB binding activity in primary effusion lymphoma (PEL) cell lines. (A) Sub-components of NF-κB activity in PEL cell lines. Nuclear extracts (1 μg) of cells were subjected to supershift analysis with indicated antibodies. (B) Effect of DHMEQ on NF-κB binding activity. PEL cell lines (TY1, BCBL1 and BC1) were treated with DHMEQ (10 μg/mL) for indicated hours. Nuclear extracts were examined for NF-κB binding activity by electrophoretic mobility shift analysis (EMSA) with a radio-labeled NF-κB-specific probe. Lower panels: results of Oct –1 probe as controls.

concentrations of DHMEQ (2.5, 5, 7.5 and 10 μg/mL). The results demonstrated a dose-dependent decrease in the cell viability for all PEL cell lines, but not for a control cell line, K562, without NF-κB activation. Peripheral blood mononuclear cells (PBMCs) and primary B-cells were shown to be resistant to DHMEQ treatment,[15,16,26] and most B-cell lines without HHV-8 or EBV were sensitive to DHMEQ when they have activated NF-κB.[16,17] The decrease in the cell viability was also time-dependent as we measured the cell viability at 24, 48, and 72 h after DHMEQ (10 μg/mL) treatment (Fig. 2). Thus, DHMEQ decreased the PEL cell viability in a dose- and time-dependent manner.

DHMEQ induced apoptosis in PEL cell lines. After 24 h of DHMEQ treatment (10 μg/mL), Annexin V reactivity was examined. Propidium iodide (PI) staining was included to discriminate the necrotic cells from apoptotic ones. Flow cytometry demonstrated a significant shift of the cell population toward Annexin V-positive areas in all cell lines, although some of the cells shifted toward PI-single positive areas (Fig. 3A). Summarized results are shown in Table 2, where results of three triplicate independent experiments are presented with the mean and SD. Furthermore, TUNEL assay demonstrated DNA fragmentation in all cell lines at 48 h (Fig. 3B). These results provided evidence for apoptosis induction by DHMEQ treatment in PEL cell lines.

DHMEQ activated both membrane and mitochondrial caspase pathways. Apoptosis can be induced via membrane and/or mitochondrial stimuli, each of which has their own specific pro-caspases to become active after receiving stimuli. Carboxy-fluorescein FLICA Apoptosis Detection Kit revealed cleaved products of caspases-3, -8, and -9 at the same time after 6 h of DHMEQ treatment (Fig. 4A). Immunoblot analyses clearly

Table 2. Quantitative results of staining primary effusion lymphoma (PEL) cell lines with Annexin V and propidium iodide (PI)

	DHMEQ	BCBL1 (%)	TY1 (%)	BC1 (%)
UL	(–)	0.71 ± 0.14	1.96 ± 1.07	0.55 ± 0.09
	(+)	7.13 ± 3.82	6.06 ± 0.50	5.04 ± 1.60
UR	(–)	1.94 ± 0.57	2.84 ± 1.92	1.96 ± 1.02
	(+)	45.92 ± 17.04	37.89 ± 15.36	38.53 ± 20.95
LL	(–)	95.37 ± 0.29	90.91 ± 4.07	93.10 ± 2.13
	(+)	34.70 ± 11.14	33.62 ± 0.82	43.58 ± 12.14
LR	(–)	1.96 ± 0.45	4.28 ± 1.61	4.37 ± 2.20
	(+)	12.34 ± 2.97	22.41 ± 14.32	12.83 ± 9.69

PEL cells incubated with or without dehydroxymethylepoxyquinomicin (DHMEQ) (10 μg/mL) for 24 h and stained with Annexing V and PI. Then, analyzed with flow cytometry. Upper left (UL), upper right (UR), lower left (LL) and lower right (LR) quadrants are responsible for PI positive only, PI and AnnexinV positive, PI and Annexin V negative, Annexin V positive only cell populations, respectively. Results are mean value ± SD of 3 triplicate independent experiments.

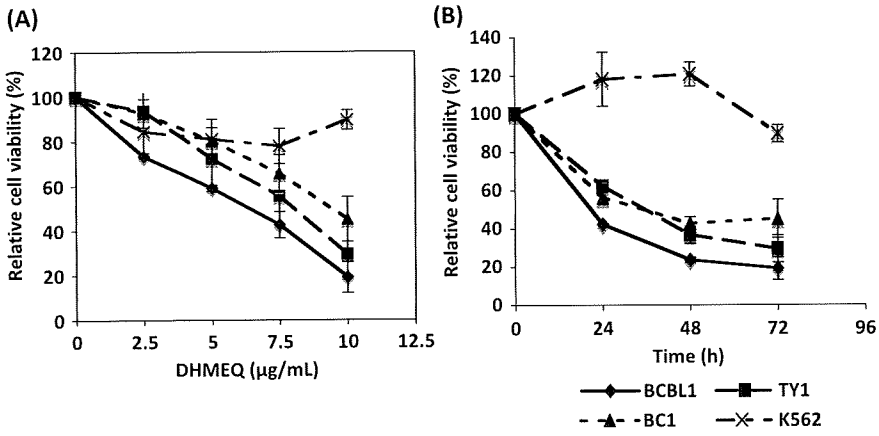

Fig. 2. Dehydroxymethylepoxyquinomicin (DHMEQ) reduced viability of primary effusion lymphoma (PEL) cells. PEL cell lines and K562 cells were treated with indicated concentrations of DHMEQ for 72 h (A) or were treated for the indicated hours with 10 μg/mL of DHMEQ (B). K562 cell line, without NF-κB activation, was used as a control. The cell viability was determined by WST-8 (Dojindo). The mean percentages of triplicate experiments compared with untreated cells are shown with standard deviation (SD).

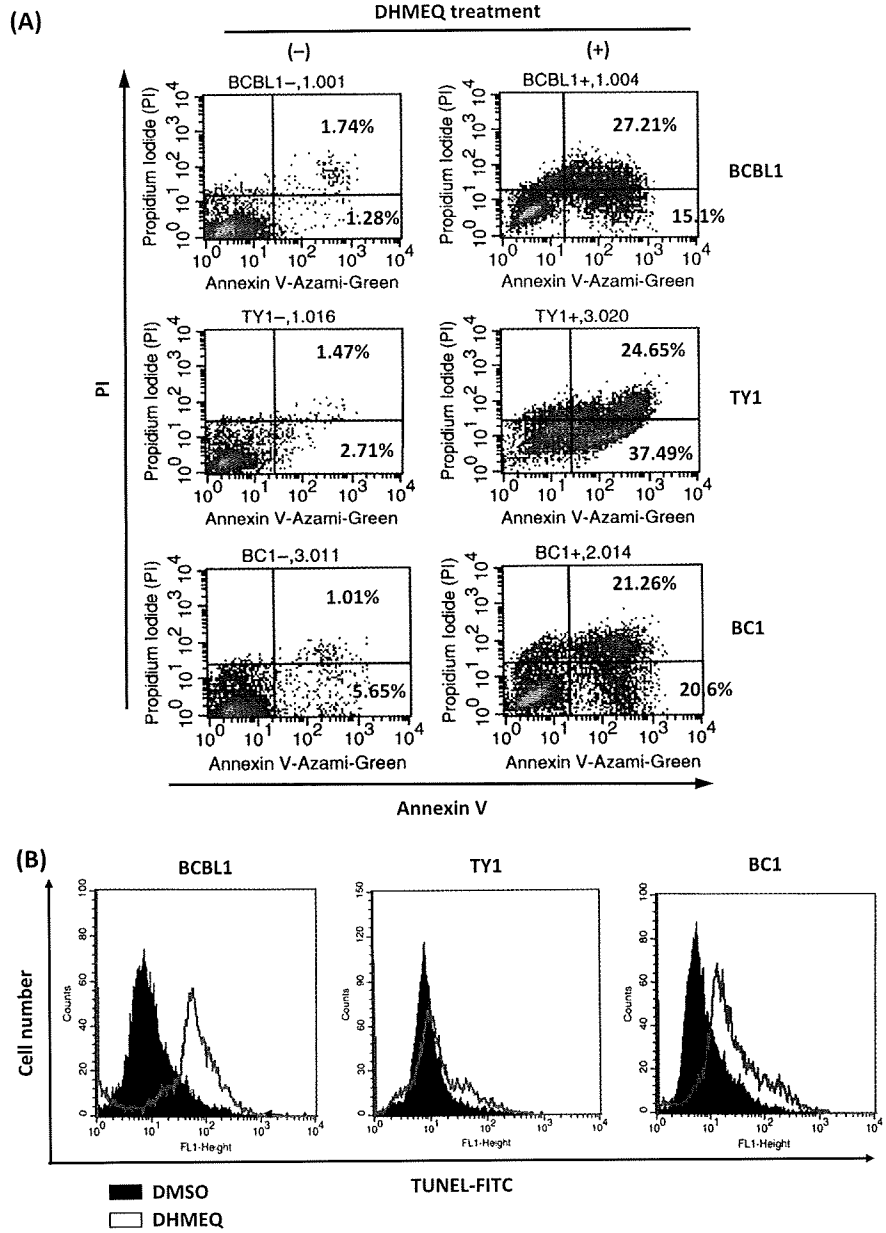

Fig. 3. Dehydroxymethylepoxyquinomicin (DHMEQ) induced apoptosis in primary effusion lymphoma (PEL) cell lines. (A) Annexin V reactivity in PEL cell lines after DHMEQ treatment. A representative result of three triplicate independent experiments is presented. PEL cell lines were treated with or without DHMEQ (10 μg/mL) for 24 h, and binding of Annexin V and intercalation of propidium iodide (PI) were analyzed by flow cytometry. (B) DNA fragmentation in the PEL cell lines after DHMEQ treatment. Terminal deoxynucleotidyl transferase-mediated dUTP nick-end labeling (TUNEL) assay was done for PEL cell lines after 48 h incubation with or without DHMEQ (10 μg/mL).

doi: 10.1111/j.1349-7006.2009.01083.x

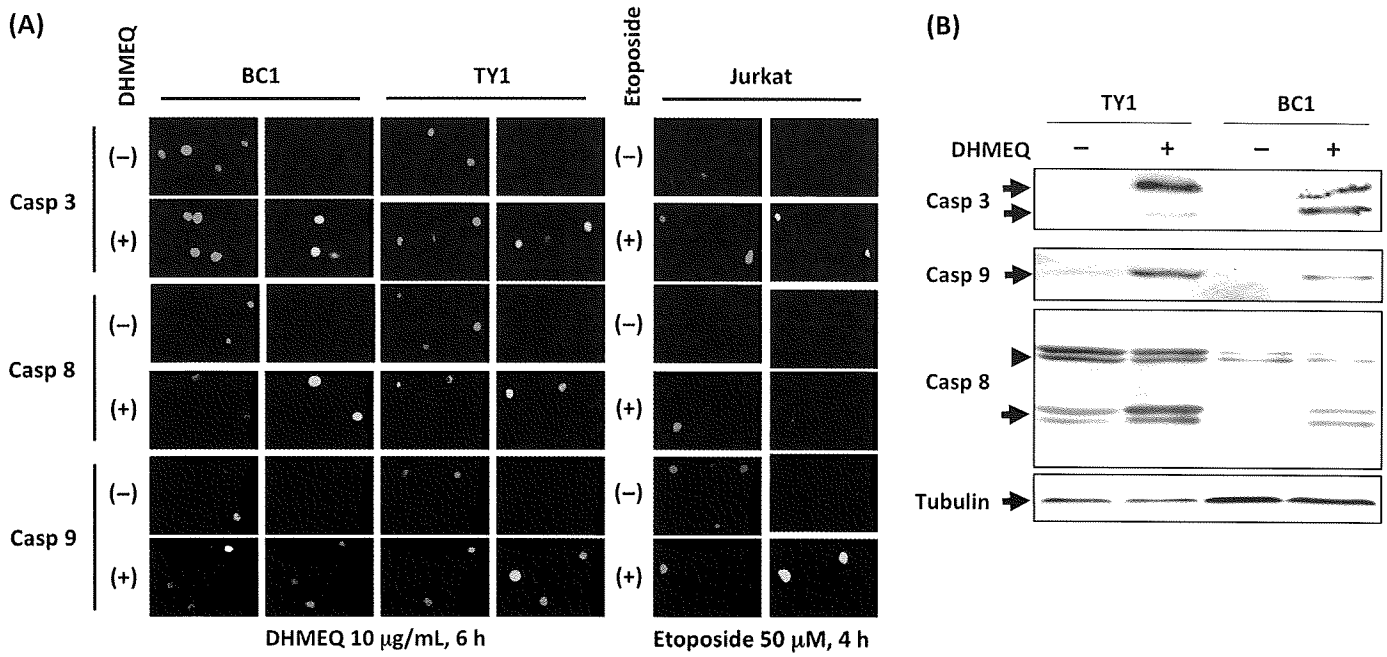

Fig. 4. Both membrane and mitochondrial caspase pathways were activated by dehydroxymethylepoxyquinomicin (DHMEQ) treatment of primary effusion lymphoma (PEL) cells. (A) Cleaved products of caspases were detected after DHMEQ treatment (10 μg/mL) for 6 h. Caspase 3, responsible for the common pathway, caspase 8, as an indicator for the membrane pathway, and caspase 9 as an indicator for the mitochondrial pathway. Jurkat cell line treated with etoposide 50 μM for 4 h served as a control. DNAs were stained by Hoechst 33258 (blue fluorescence). Green fluorescence indicated cleaved products of caspases bound to FLICA peptides. (B) Immunoblot analysis of caspase cleavage. TY1 and BC1 cells were treated with 10 μg/mL of DHMEQ for 6 h. Samples of 30 μg of whole cell lysates were examined. Positions of cleaved forms of caspase 3 and 9 are indicated on the left of the upper two panels (arrows). In the third panel, uncleaved and cleaved forms of caspase 8 are indicated on the left (arrowhead: uncleaved). An immunoblot of α-tubulin served as a control (bottom panel).

demonstrated production of cleaved products of caspase-3, -8 and -9 at the same time after 6 h of DHMEQ treatment (Fig. 4B).

Taken together, the results suggested that both caspase pathways became active in the PEL cell lines as a result of incubation with DHMEQ for 6 h.

DHMEQ modulated NF-κB target genes, apoptotic and cell cycle regulating genes. Whole human genome expression analysis was done to obtain a comprehensive view of DHMEQ effect on PEL cell lines, and to confirm the efficient targeting of the NF-κB pathway. DHMEQ down- or up-regulated expression levels of 72 and 71 genes, respectively, in BC1 and BCBL1 cell lines (Fig. 5A). Down-regulation was observed in NF-κB target genes, such as *IL6*, *Myc*, *CCR5*, *BCL-xL*, *cIAP2* and *NF-κB1*. *Bcl-xL*, *c-IAP2*, and *NF-κB1* are also anti-apoptotic genes. Other anti-apoptotic genes, such as *Birc5* and *IGF1R*, were down-regulated. However, some anti-apoptotic genes including *SSP1*, *VEGF*, *MIF* and *BAG3* were up-regulated. Some of pro-apoptotic genes such as *DEDD2*, *CDKN1A* and *APOE* were up-regulated, whereas *TNFSF10* was down-regulated. Most of the genes involved in cell cycle arrest were up-regulated, the examples of which were *CDKN1A*, *CDKN1B*, *PPP1R15* A and *DDIT3* (Supporting Information).

For validation of above results, we performed real-time RT-PCR analysis. For this purpose, we selected three up-regulated and three down-regulated genes. The results provided evidence that validate the results of expression array analysis, showing up- or down-regulation of the selected genes (Fig. 5B). Furthermore, the levels of up- or down-regulation appeared to well correlate with those obtained by the expression array analysis described above.

Since the genes involved in cell cycle arrest were induced by DHMEQ, we next examined effects of DHMEQ treatment on the cell cycle regulating using three cell lines. The results showed significant accumulation of the cells in G2/M phase at 6 h of treatment (Fig. 5C,D).

Gene ontology analysis on the genes the expression levels of which were significantly altered by the addition of DHMEQ in BC1 cells (P-value < 0.01) revealed that the majority of the genes in the following categories were down-regulated: (i) negative regulators of NF-κB import to the nucleus; (ii) IκB kinase and NF-κB cascade; (iii) negative regulators of apoptosis; (iv) DNA repair; and (v) cell cycle checkpoint. In contrast, the majority of the genes in the following categories were up-regulated: (i) positive regulators of apoptosis; (ii) cell cycle arrest; and (iii) regulators of cyclin-dependent protein kinase activity (Fig. 5E).

Taken together, we observed a trend toward induction of pro-apoptotic and cell cycle arrest genes, concomitant with suppression of NF-κB target, anti-apoptotic and DNA repair genes.

DHMEQ did not induce HHV-8 reactivation. Semi-quantitative RT-PCR was done to examine changes in the viral gene expression after the DHMEQ treatment. Some viral genes known as 'lytic genes' were selected as well as those with important viral functions. The results demonstrated low or undetectable levels of lytic gene expression without significant changes until 14 h of treatment, suggesting that NF-κB inhibition by DHMEQ treatment did not lead to viral production in these cells (Fig. 6). Expression levels of *v-FLIP*, *v-cyclin*, and *LANA* were slightly up-regulated after 3–6 h of DHMEQ treatment, returning to the basal levels after 14 h. It is worthy of note that *v-FLIP*, a potent viral activator of NF-κB pathway, showed almost constant levels of expression irrespective of DHMEQ treatment. Taken together, we could not obtain evidence for induction of virus proliferation that was previously reported as an effect of NF-κB inhibition in PEL cell lines.[31]

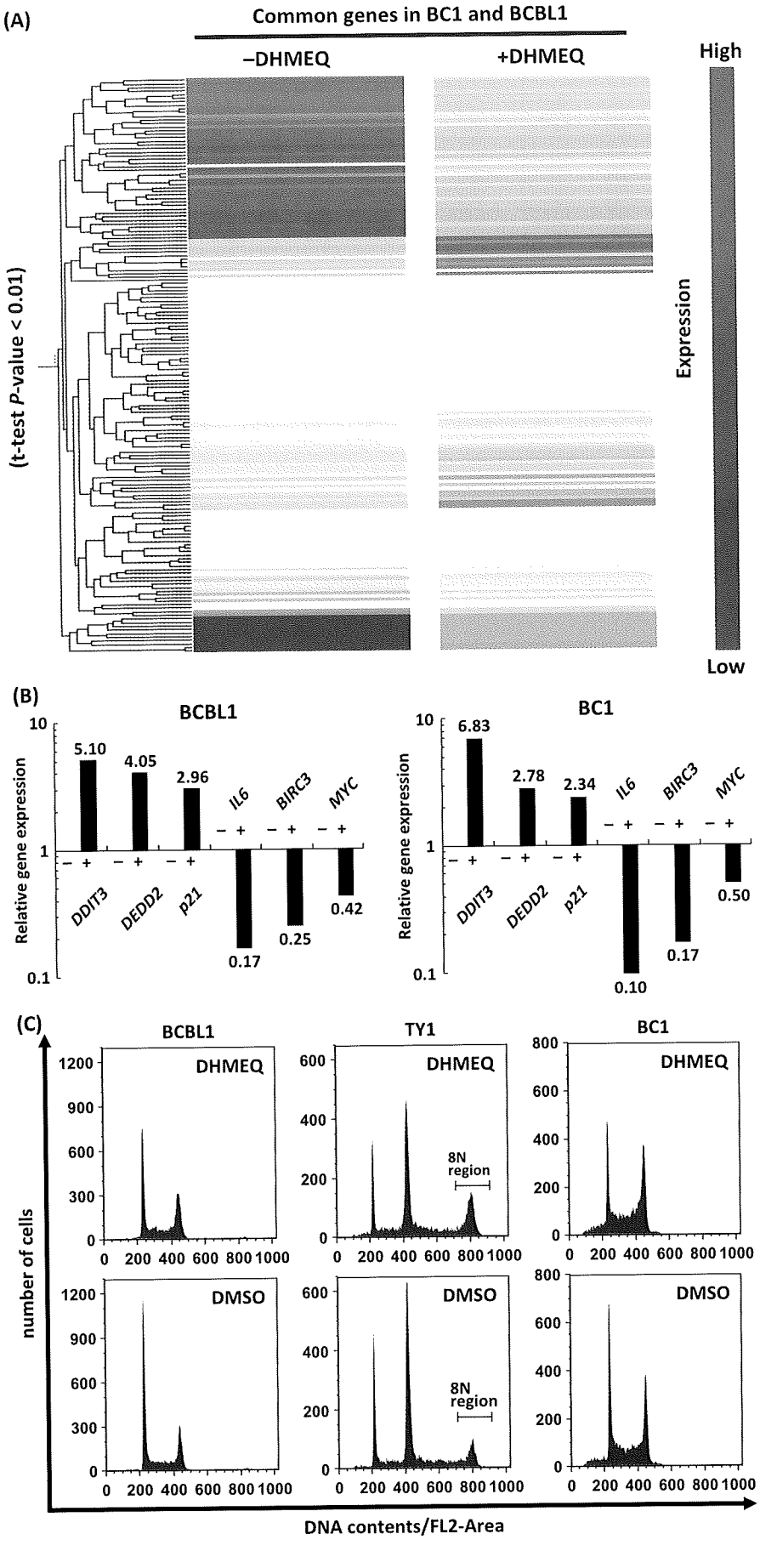

Fig. 5. Dehydroxymethylepoxyquinomicin (DHMEQ) modulated genes responsible for proliferation, cell cycle, pro- and anti-apoptosis. Whole Human Genome Oligo Microarray Kit (Agilent Technologies) was used to evaluate the gene expression in BC1 and BCBL1 with or without DHMEQ (10 μg/mL), 6 h. (A) The result of cluster analysis showed significant changes in expression levels between ±DHMEQ in both cell lines (*t*-test, *P*-value < 0.01). (B) Results of real-time reverse-transcription–polymerase chain reaction for validation of the array data. Up- or down-regulation of selected genes was confirmed in both cell lines tested. (C) Effects on cell cycle regulation. Representative results of flow cytometry after 6 h of DHMEQ are presented. TY1 cells appear to be a mixture of 2 N and 4 N populations. (D) Percentages of cells in G2/M phase. In TY1 cells, the percentage of the 8 N region was considered to represent a significant part of the cells at G2/M, and was used for comparison. Differences were statistically significant (*1, $P < 0.05$, *2, $P < 0.05$, *3, $P < 0.001$) (E) Gene ontology analysis on BC1 genes of which expression levels were significantly changed by addition of DHMEQ (*t*-test, *P*-value < 0.01). The graph shows numbers of the genes in following selected categories: a, negative regulators of NF-κB import into nucleus; b, IκB kinase and NF-κB cascade; c, positive regulators of apoptosis; d, negative regulators of apoptosis; e, DNA repair; f, cell cycle arrest: g, cell cycle checkpoint; h, regulators of cyclin dependent protein kinase activity. Positive and negative areas represent the number of up-regulated genes, and those of down-regulated genes, respectively.

doi: 10.1111/j.1349-7006.2009.01083.x

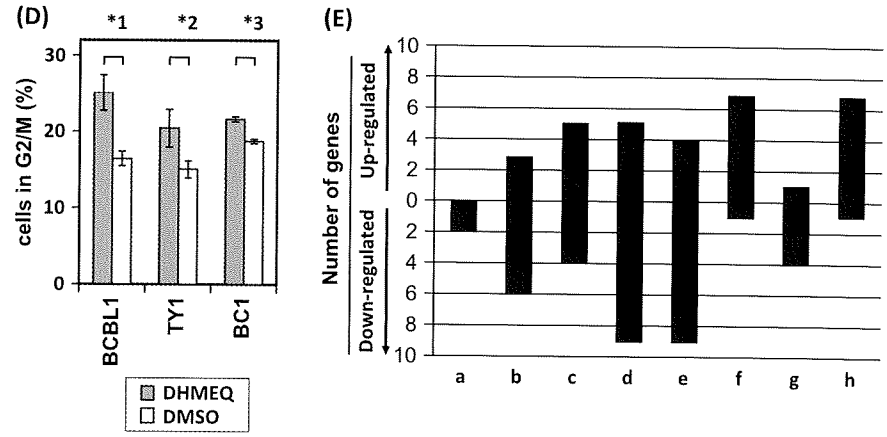

Fig. 5. Continued

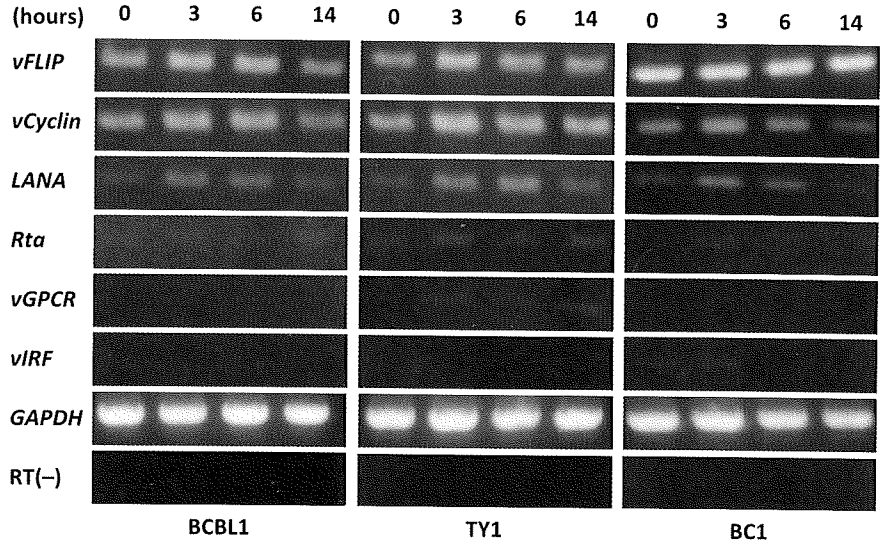

Fig. 6. Viral gene expression after dehydroxymethylepoxyquinomicin (DHMEQ) treatment showed no transition from latent to lytic phase. Viral gene expression after DHMEQ treatment (10 μg/mL) at different time points was examined by semiquantitative reverse-transcription–polymerase chain reaction. Two micrograms of total RNA were used to prepare cDNA using oligo(dT)$_{12-18}$ primer. *GAPDH* and RT(–) served as controls.

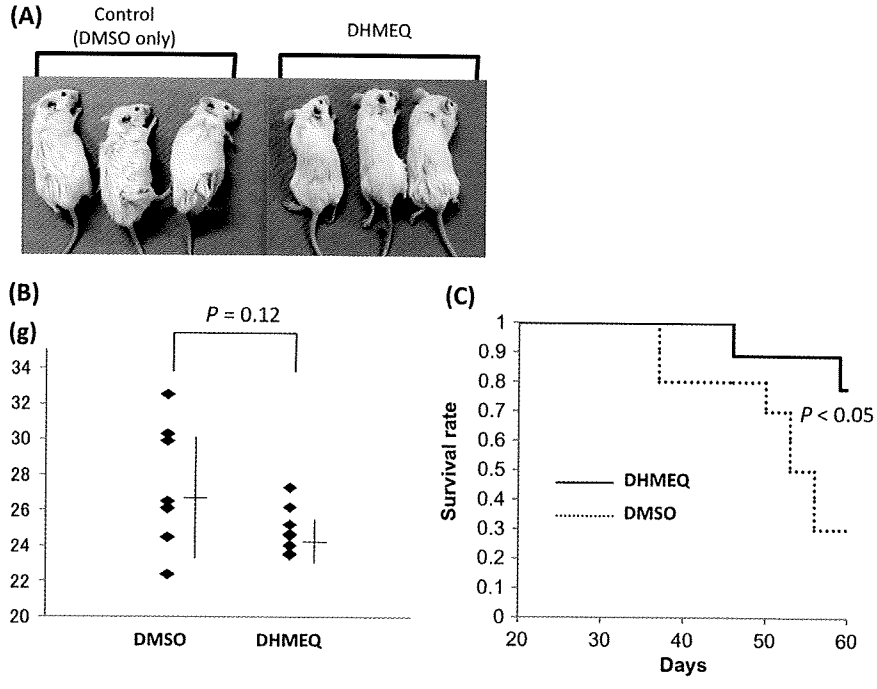

Fig. 7. Dehydroxymethylepoxyquinomicin (DHMEQ) rescued primary effusion lymphoma (PEL) xenografted mice. Mice at 5 weeks old were injected with 4×10^6 TY 1 cells intraperitoneally. DHMEQ (8 mg/kg) in 0.5% CMC was administered three times a week intraperitoneally for 1 month. Dimethyl sulfoxide in 0.5% CMC was administered to the control group. (A) Gross appearances of the mice. (B) A graph showing weights of mice with mean values. (C) Survival curves of mice with or without DHMEQ treatment.

DHMEQ showed a potent inhibitory effect on the growth of PEL cells in SCID mice. We next examined whether DHMEQ treatment could be effective against xenografted tumors in a SCID mice model. TY1 cells were injected intraperitoneally into the SCID mice and DHMEQ or vehicle alone was administered according to the protocol described in the Materials and Methods section. The gross appearance of the mice with or without DHMEQ treatment was significantly different, showing abdominal distention in vehicle-treated mice, whereas DHMEQ-treated mice were apparently normal in body shape. The body weights of the DHMEQ-treated mice were much less than those of vehicle-treated mice after 1 month, although the difference was not statistically significant (Fig. 7A,B). DHMEQ treatment rescued 8/10 xenografted mice at the point of 3 months, whereas only 3/10 survived in the vehicle-treated control group. The results are similar to those of our previous experiments in animal models of adult T-cell leukemia (ATL).[32,33] Statistical analysis showed a significant increase in the survival rate in the mice treated with DHMEQ compared with the control (Cox-Mantel test; $P < 0.05$, Fig. 7C). These results demonstrated that DHMEQ was effective against PEL cells *in vivo*, which provided supportive evidence for possible clinical application.

Discussion

The present work demonstrated that DHMEQ transiently abrogated the NF-κB activation in PEL cell lines with significant recovery of NF-κB activity after 24 h. Apoptotic cell death was observed in a few days without reactivation of HHV-8. Furthermore, DHMEQ rescued PEL-xenografted SCID mice preventing formation of tumors and effusions. Thus, we suggest DHMEQ as a promising candidate for molecular targeted therapy of the PEL.

NF-κB activity recovered significantly after 24 h of DHMEQ-treated PEL cell lines, which was not observed in other lymphoid cell lines we have so far tested,[16–18] although low levels of NF-κB recovery were observed after 24 h or later (unpublished observation). Thus, the rapid and significant recovery of NF-κB activity can be considered as a characteristic of PEL cell lines. Transient NF-κB inhibition can be an advantage for DHMEQ compared with other NF-κB inhibitors, since persistent inhibition of the NF-κB pathway may lead to adverse effects on innate and acquired immune systems where NF-κB plays a pivotal role. The mechanism for recovery of the NF-κB activity remains to be studied. It may be due to degradation of DHEMQ within the cells and/or persistence of the NF-κB activating stimuli that can overcome the effects of DHMEQ. No information is available at present as to the half-life of DHMEQ in the cell. On the other hand, persistence of high levels of NF-κB activating signals may be explained by v-FLIP, a well-known viral stimulator of the NF-κB pathway,[7,34,35] that was expressed at stable levels irrespective of DHMEQ treatment (Fig. 6).

Another benefit of DHMEQ may reside in targeting the translocation of p65 into nuclei. Generally, target specificity of kinase inhibitors is not strict. For example, Bay11-7083 has non-specific activities on other kinases along with tyrosine phosphorylation of a protein of unknown origin.[36] Furthermore, Bay11-7085 does not inhibit translocation of p65 into nuclei, and shows non-specific inhibition of binding of other transcription factors to its binding sequences.[37] On the other hand, DHMEQ treatment results in disappearance of p65 and p50 in the nuclei of cell lines of Hodgkin-Reed-Sternberg (H-RS) cells and ATL, not affecting binding of other transcription factors such as AP-1 and Oct1 in EMSA.[15,16] Taken together, the specific activity of DHMEQ appears to be an advantage over other NF-κB inhibitors with respect to avoiding adverse effects.

The apoptosis cascade was triggered with transient abrogation of NF-κB by DHMEQ treatment. Furthermore, subsequent recovery of NF-κB activity could not rescue the DHMEQ-treated PEL cells, suggesting that DHMEQ triggered irreversible activation of the apoptosis cascade. These observations are in line with those discussed in the context of 'oncogene addiction' and 'oncogenic shock'.[38–40] Sharma *et al.* proposed a model referred to as 'oncogenic shock' to account for the observed apoptotic outcome resulting from the acute inactivation of oncoproteins in addicted cancer cells. According to this model, proapoptotic as well as prosurvival signals are both outputs emanating from the same addicting oncoprotein, and the differential decay rates associated with these two broad classes of signals following oncoprotein inactivation, leads to a signal imbalance that contributes to cell death.[39,40] The results of our gene ontology analyses demonstrated that more anti-apoptotic genes are down-regulated at 6 h compared with pro-apoptotic genes (Fig. 5B), which suggest a condition after acute inactivation of the oncoprotein, where rapid attenuation of oncoprotein-generated prosurvival signals is associated with lingering pro-apoptotic signals.

The pathway analysis of apoptosis revealed activation of both membrane and mitochondrial pathways, which is evidenced by detection of cleaved products of caspases-8 and -9 at the same time. Previously we reported the same results using human T-cell leukemia virus type I-transformed cells and cell lines of H-RS cells and multiple myeloma.[15,16,18] Since links between the receptor and the mitochondrial pathways exist at different levels, upon death receptor triggering, activation of caspase-8 may result in cleavage of Bid, a Bcl-2 family protein with a BH3 domain only, which in turn translocates to mitochondria to release cytochrome c thereby initiating a mitochondrial amplification loop.[41,42] In addition, cleavage of caspase-6 downstream of mitochondria may feed back to the receptor pathway by cleaving caspase-8.[43] Thus, the data can be interpreted in either context, leaving the exact mechanism of DHMEQ-induced apoptosis remaining to be studied.

DHMEQ did not induce transition from the latent to lytic phase of HHV-8 (Fig. 6). There are controversies as to whether inhibition of NF-κB leads to replication of HHV-8,[31] or not.[10] Another investigator suggested that NF-κB is necessary for HHV-8 replication.[44] However, we did not find any significant differences in the expression of known lytic genes after NF-κB inhibition (Fig. 6). Thus, our results did not support the idea that DHMEQ administration may increase the risk for viral replication. Furthermore, the latent viral genes such as *LANA*, *v-FLIP*, or *v-cyclin* did not show significant changes in the levels of gene expression. RNA interference results showed that v-FLIP is essential for the survival of PEL cells.[8] Our data indicated that NF-κB activation, not v-FLIP itself, was essential for survival of PEL cells, since apoptosis was induced in the presence of stable levels of v-FLIP expression.

Inhibition of NF-κB causes profound effects on cellular gene expression by direct and indirect mechanisms. The results of expression array analysis confirmed down-regulation of many NF-κB target genes, which was mostly in accordance with previously reported results of NF-κB inhibition by Bay11-7082 in EBV-infected lymphoblastoid cell lines.[45] Although the suppressions of *IL6* and *cIAP2* were observed previously by using Bay11-7082 on a PEL cell line,[10] we could not find significant suppression in *c-FLIP*, *cIAP1*, *TRAF2* or *IκBα* as they reported. Instead, we found *Bcl-xL*, *Myc*, *CCR5*, *NF-κB1* and *FAS* among the down-regulated genes. These differences could be due to different agents used, with different specificity of activities. Suppression of other anti-apoptotic or cell cycle progression genes could be mediated by the functions of other genes, which were modulated by NF-κB inhibition. The result of gene ontology biological process analysis of the genes with significant changes in expression levels were reasonable because it showed a trend toward induction of pro-apoptotic and cell cycle

doi: 10.1111/j.1349-7006.2009.01083.x